

**EFFECT OF CRYOROLLING ON MECHANICAL AND FATIGUE  
CRACK GROWTH BEHAVIOR OF AL ALLOY 6351**

**A DISSERTATION**

*Submitted in partial fulfillment of the  
Requirements for the award of the degree*

*of*

**MASTER OF TECHNOLOGY**

*in*

**MECHANICAL ENGINEERING**

**(With Specialization in Machine Design Engineering)**

*by*

**GAYANENDRA SAINI**

**(17539004)**



**DEPARTMENT OF MECHANICAL AND INDUSTRIAL ENGINEERING  
INDIAN INSTITUTE OF TECHNOLOGY ROORKEE**

**ROORKEE-247667 (INDIA)**

**MAY, 2019**



# INDIAN INSTITUTE OF TECHNOLOGY ROORKEE, ROORKEE

## CANDIDATE'S DECLARATION

I hereby declare that the work carried out in this report entitled “**Effect Of Cryorolling On Mechanical And Fatigue Crack Growth Behavior Of Al Alloy 6351**”, is presented on behalf of partial fulfillment of the requirement for the Dissertation of “**Master of Technology**” in mechanical engineering with specialization in **Machine Design Engineering** submitted to Department of Mechanical and Industrial Engineering, Indian Institute of Technology Roorkee under the supervision of **Prof. I.V. Singh** and **Prof. B.K. Mishra**, Professors, Department of Mechanical and Industrial Engineering, Indian Institute of Technology Roorkee.

Date:

Place: Roorkee

(**Gayanendra Saini**)

## CERTIFICATE

This is to clarify that the above statement made by the candidate is correct to the best of my knowledge and belief.

(**Prof. I.V. Singh**)  
Professor  
MIED, IIT Roorkee

(**Prof. B.K. Mishra**)  
Professor  
MIED, IIT Roorkee

## ABSTRACT

---

Mechanical and fatigue behavior of Al alloy has studied after cryorolling (CR) in this experimental project. The Al alloy is heated to temperature 540°C and hold approximately for two hours and quenched into water to form supersaturated solid solution in alpha phase. Heat treated and quenched alloy is called solution treated or bulk alloy (ST). Cryorolling is done at extremely low temperature using liquid nitrogen and four different cases (with 20 % reduction, 40 % CR, 60 % CR and 80 % CR) are taken to calculate the Yield strength (YS), ultimate tensile strength (UTS), hardness and fatigue crack growth rate in AL alloy 6351. To study the microstructure of 6351 alloy Field Emission Scanning Electron Microscopy (FESEM), X-Ray Diffraction (XRD) and optical microscope are used. The cryorolled alloy produced ultrafine grains (ufg) which improve mechanical properties (YS, UTS and Hardness) and fatigue crack growth resistance but simultaneously reduce ductility. To optimize mechanical and fatigue properties aging treatment of Al 6351 is done for temperature range 100°C to 200°C and optimum mechanical and fatigue properties are found at aging temperature and time of 100°C and 12 hours. The yield strength (Y.S), ultimate tensile strength (U.T.S) and hardness (365 Mpa, 415 Mpa and 170 Hv) for 80 % CR alloy increased as compared to the bulk 6351 Al alloy (YS-140 MPa, UTS-202 MPa and hardness 67 Hv). The cryorolled Al alloy shows higher mechanical properties as compare to bulk or solution treated alloy. It is due to increase in dislocation density and suppression of dynamic recovery and production of ultrafine grains. Fatigue crack growth resistance of cryorolled samples also improve as compare to solution treated alloy it is due to increase the number of grain boundaries produce through cryorolling and formation of finer precipitates of magnesium silicide ( $Mg_2Si$ ) and interaction between propagating crack and grain boundaries.

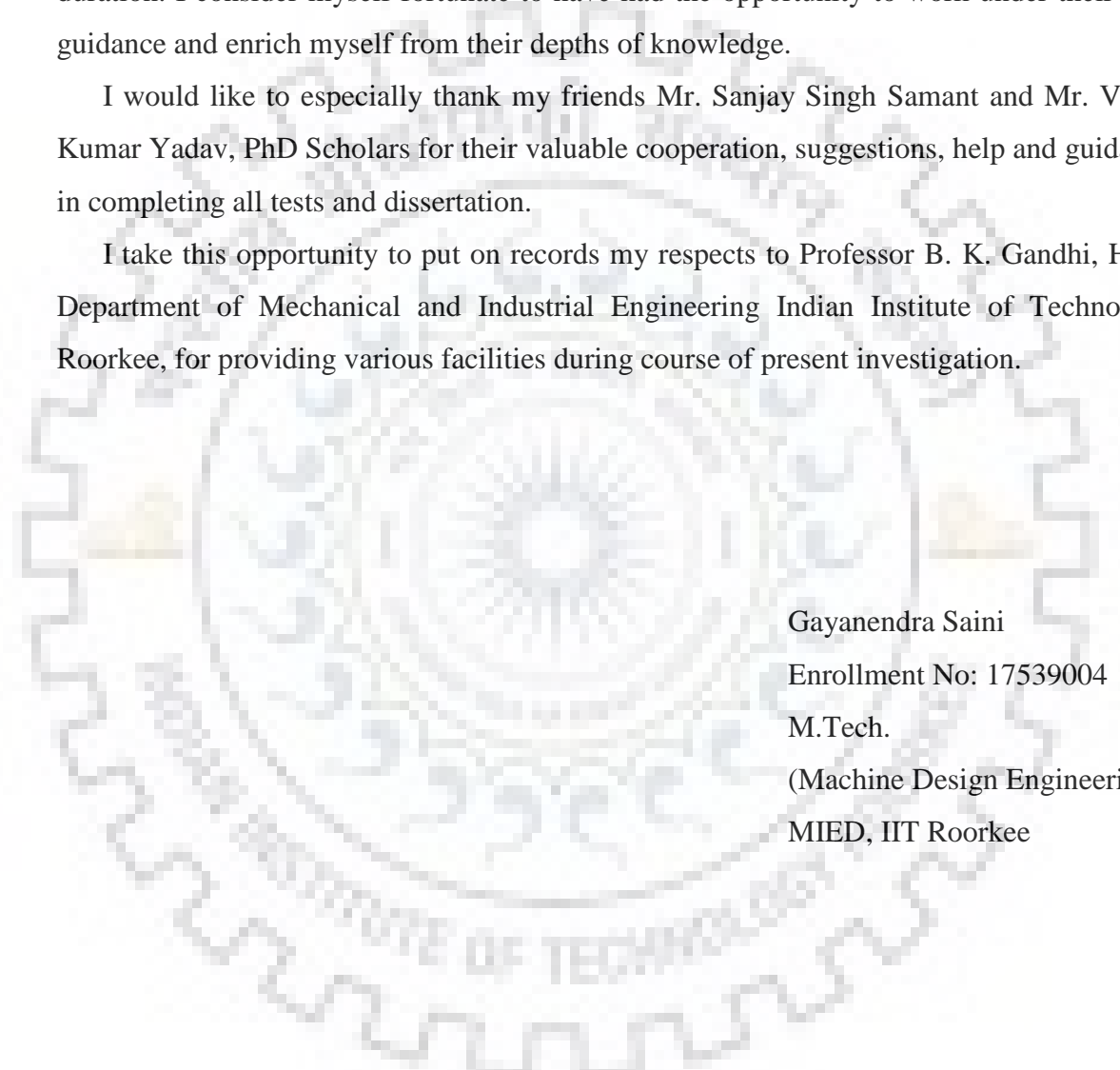
## ACKNOWLEDGEMENTS

---

I wish to express a deep sense of gratitude and sincere thanks to my supervisor Prof. I.V. Singh and Prof. B.K. Mishra, Professors, Department of Mechanical and industrial engineering Indian Institute of Technology Roorkee, Roorkee for their invaluable inspiration, wholehearted Co-operation, motivation and important assistances throughout the duration. I consider myself fortunate to have had the opportunity to work under their able guidance and enrich myself from their depths of knowledge.

I would like to especially thank my friends Mr. Sanjay Singh Samant and Mr. Vinay Kumar Yadav, PhD Scholars for their valuable cooperation, suggestions, help and guidance in completing all tests and dissertation.

I take this opportunity to put on records my respects to Professor B. K. Gandhi, HOD Department of Mechanical and Industrial Engineering Indian Institute of Technology Roorkee, for providing various facilities during course of present investigation.



Gayanendra Saini  
Enrollment No: 17539004  
M.Tech.  
(Machine Design Engineering)  
MIED, IIT Roorkee

## TABLE OF CONTENTS

<b>Title</b>	<b>Page</b>
<b>CANDIDATE'S DECLARATION</b>	<b>i</b>
<b>ABSTRACT</b>	<b>ii</b>
<b>ACKNOWLEDGEMENTS</b>	<b>iii</b>
<b>TABLE OF CONTENTS</b>	<b>iv</b>
<b>LIST OF FIGURES</b>	<b>vi</b>
<b>LIST OF TABLES</b>	<b>viii</b>
<b>Chapter 1</b> .....	<b>1</b>
<b>INTRODUCTION AND LITERATURE REVIEW</b> .....	<b>1</b>
1.1 INTRODUCTION .....	1
1.2 LITERATURE REVIEW .....	3
1.3 SCOPE OF WORK .....	5
1.4 OBJECTIVE OF CURRENT WORK .....	6
<b>Chapter 2</b> .....	<b>7</b>
<b>EXPERIMENTAL PROCEDURE</b> .....	<b>7</b>
2.1 MATERIAL SELECTION .....	7
2.2 CRYOROLLING .....	7
2.2.1 Advantage of Cryorolling .....	8
2.2.2 Disadvantage of Cryorolling .....	8
2.3 PURPOSE OF CRYOROLLING .....	9
2.3.1 Grain Size .....	9
2.2.3 Dislocation Density .....	9
2.2.4 Suppression of Dynamic Recovery .....	9
2.3 ROOM TEMPERATURE ROLLING .....	9
2.4 EXPERIMENTAL SET UP FOR CRYOROLLING .....	9
2.5 CRYOROLLING PROCEDURE .....	11
2.6 MICROSTRUCTURE CHARACTERIZATION .....	12
2.6.1 Optical Microscopy .....	12
2.6.2 Field Emission Scanning Electron Microscope (FE-SEM) .....	13
2.6.3 X-Ray Diffraction .....	14
2.7 MECHANICAL TESTING PROCEDURE .....	15
2.7.1 Tensile Testing .....	15

2.7.2 Hardness Testing.....	16
2.7.3 Fatigue Crack Growth Testing .....	17
<b>Chapter 3 .....</b>	<b>19</b>
<b>MECHANICAL BEHAVIOR AND CHARACTERIZATION.....</b>	<b>19</b>
3.1 INTRODUCTION.....	19
3.2 MICROSTRUCTURE CHARACTERIZATION .....	19
3.2.1 Optical Microscopy .....	19
3.2.2 EDAX Analysis Using FE-SEM.....	21
3.2.3 X Ray Diffraction Analysis.....	27
3.3 MECHANICAL BEHAVIOR .....	28
3.3.1 Tensile Test .....	28
3.3.2 Micro Hardness Testing.....	30
3.3.3 Effect of Aging on Mechanical Properties.....	35
3.4 Fractography .....	39
3.4.1 Tensile Surface Fractography .....	39
<b>Chapter 4 .....</b>	<b>41</b>
<b>FATIGUE CRACK GROWTH BEHAVIOR.....</b>	<b>41</b>
4.1 INTRODUCTION.....	41
4.2 FATIGUE CRACK GROWTH (FCG).....	42
4.3 FCG TEST PROCEDURE.....	43
4.3.1 Fatigue Pre-cracking .....	43
4.3.2 K decreasing.....	43
4.3.3 K increasing .....	44
4.3.4 Constant Load Test .....	44
4.4 FATIGUE CRACK GROWTH TEST OF 6351 AL ALLOY .....	44
4.5 FATIGUE CRACK GROWTH FRACTOGRAPHY .....	47
<b>Chapter 5 .....</b>	<b>49</b>
<b>CONCLUSION AND FUTURE SCOPE.....</b>	<b>49</b>
5.1 CONCLUSION .....	49
5.2 FUTURE SCOPE.....	49
<b>REFERENCES.....</b>	<b>52</b>

## LIST OF FIGURES

Figure		Page
2.1	Sample of 6351 Al alloy before cryorolling.....	8
2.2	Sample of 6351 Al alloy after cryorolling.....	8
2.3	Cryorolling machine .....	10
2.4	Liquid nitrogen setup .....	10
2.5	Schematic diagram of cryorolling process.....	12
2.6	Optical microscope.....	13
2.7	Optical micrograph samples.....	13
2.8	FE-SEM QUANTA 200 FEG.....	14
2.9	XRD machine.....	14
2.10	Power hacksaw machine.....	15
2.11	Geometry of Tensile specimen.....	16
2.12	Tensile specimen.....	16
2.13	Micro hardness samples.....	17
2.14	Mitutoyo hardness tester.....	17
2.15	Geometry of compact specimen for FCG.....	18
2.16	Compact Specimen for FCG.....	18
3.1	Optical micrograph of 6351 Al alloy.....	20
3.2	SEM micrograph with EDX analysis for ST Al 6351 alloy.....	22
3.3	SEM micrograph with EDX analysis of 20 % cryorolled 6351 alloy.....	23
3.4	SEM micrograph with EDX analysis of 40 % cryorolled 6351 alloy.....	24
3.5	SEM micrograph with EDX analysis of 60 % cryorolled 6351 alloy.....	25
3.6	SEM micrograph with EDX analysis of 80 % cryorolled 6351 alloy.....	26
3.7	XRD analysis .....	27
3.8	Engineering stress vs Plastic Strain Plot at room temperature.....	29
3.9	UTS, US and Elongation of ST, CR 20, CR 40 and CR 60 Al alloy 6351.....	30
3.10	The hardness value of ST, CR 20, CR 40, CR 60 and CR 80 Al alloy.....	33
3.11	The variation of hardness value of 20 % CR Al 6351 alloy with temperature and time.....	33
3.12	The variation of hardness value of 40 % CR Al 6351 alloy with temperature and time.....	34

3.13	The variation of hardness value of 60 % CR Al 6351 alloy with temperature and time.....	34
3.14	The variation of hardness value of 80 % CR Al 6351 alloy with temperature and time.....	35
3.15	Stress vs plastic strain curve of 40 % CR 6351 alloy at various temperature and aging time.....	36
3.16	Stress vs plastic strain curve of 60 % CR 6351 alloy at various temperature and aging time.....	37
3.17	Stress vs plastic strain curve of 80 % CR 6351 alloy at various temperature and aging time.....	38
3.18	Optimum properties (YS, UTS and Elongation) of 6351 Al alloy.....	39
3.19	Tensile fractographs of 6351 Al alloy.....	41
4.1	Fatigue crack growth curve.....	42
4.2	Crack length versus cycles curve.....	43
4.3	FCG curve of ST, CR 40, CR 60 and CR 80 AL alloy 6351.....	46
4.4	Crack length v/s number of cycles curve.....	48
4.5	Fatigue crack growth fractographs.....	49



## LIST OF TABLES

<b>Table</b>		<b>Page</b>
2.1	Chemical composition of Al 6351 alloy.....	8
3.1	UTS, YS and Elongation of 6351 Al alloy at room Temperature.....	31
3.2	Hardness for Al 6351 alloy at room temperature.....	32
3.3	Hardness and Aging time for 20 % CR Al 6351 alloy.....	32
3.4	Hardness and Aging time for 20 % CR Al 6351 alloy.....	33
3.5	Hardness and Aging time for 20 % CR Al 6351 alloy.....	33
3.6	Hardness and Aging time for 20 % CR Al 6351 alloy.....	33
3.7	YS, UTS and Aging time for 40 % CR Al 6351 alloy.....	38
3.8	YS, UTS and Aging time for 40 % CR Al 6351 alloy.....	39
3.9	YS, UTS and Aging time for 40 % CR Al 6351 alloy.....	40
3.10	Value of Paris constants (C, m) for Al 6351 alloy.....	48

# INTRODUCTION AND LITERATURE REVIEW

---

## 1.1 INTRODUCTION

Aluminium is the third largest available metal after oxygen and silicon and it is represented by chemical symbol Al and has atomic number 13. Al alloys are obtained by adding different chemical elements which provide strength to pure Aluminium. Al alloy are widely used metal in form of wrapping foil and other structural and engineering application. Al alloys are widely used due to its light weight and good corrosion resistance. The main component of aluminium alloy are copper, magnesium, manganese, silicon, tin and zinc. These alloys are classified into two broad categories, first one casting alloys and second wrought alloys. These two alloys further subdivided into heat-treatable and non-heat-treatable alloys. More than 80 % of aluminium is used in form of wrought product like as rolled plate, foils and extruded bars, channels, beam. Almost all cast aluminium alloy have two main constituents namely aluminium and silicon in which silicon has found in the range of 4 to 13 %. The main function of silicon is to provide casting properties.

More than 80 % of mechanical failure cause by fatigue failure. Our objective to find out how materials fail and how crack is generated in the materials and how it is propagated through the materials. Ultimately, we want to improve the mechanical and fatigue properties of the Al alloy 6351 through cryorolling and heat treatment process to prevent such failures. Fatigue is type of failure in which material is failed due to repeated applied loads. It is the localized phenomenon in which crack is generated either inside or outside surface of material. Fatigue occurs well below the yield strength or ultimate strength of material. If the applied loads are less than threshold value, then microscopic cracks will start to form at the surface or inside the material depending upon where stress is maximum. When crack will reach its critical limit then it propagates suddenly and then structure is failed. Fatigue failures behave as a brittle fracture. There are many factors which affect the fatigue life of component, material and structure e.g. shape of component, surface finish etc.

Fatigue life is defined as the number of stress cycles that a specimen sustains before fracture. Ferrous material like steel, titanium shows well defined endurance limit below the material can sustain infinite number of cycles ( $5 \times 10^8$ ) without failure. Fatigue limit also called endurance strength or fatigue strength. Non-ferrous alloys do not show well defined endurance limit. S-N curve is obtained from a rotating beam test where many samples is used

to reach the endurance limit of metals. There are various factors which are used to describe the mechanical fatigue such as cyclic load, stress intensity, fatigue crack growth rate, ratio factor. The ratio factor is defined as the ratio of minimum force  $P_{min}$  to maximum force  $P_{max}$ . The stress intensity factor  $K$ , at crack tip, is calculated from applied load. In metals which have no macroscopic and microscopic discontinuities. Fatigue process starts at surface where extrusion and intrusion are formed due repetitive applied loads, these intrusion and extrusion act as sites for crack generation. Fatigue process can also begin at macroscopic discontinuities, microscopic discontinuities at grain scale and fatigue can also starts parts having common design features e.g. notch, holes, change in cross- section, keyways.

Al-Mg-Si Wrought alloys (6xxx series aluminium alloys) are generally used for structural engineering applications in aerospace and automotive industries, and in civil engineering due to their high strength to weight ratio, good formability, reasonable weldability, high corrosion resistance, and lower cost. Al 6351 alloy has light weight ( $\rho=2.7g/cm^3$ ) and high corrosion resistance to any environment rather humid or chemical environment. This alloy has good Electrical and thermal conductivity which is 4 times greater than that of steels. Its chemical compositions are Si (0.93), Fe (0.36), Cu (0.1), Mn (0.57), Mg (0.55), Zn (0.134), Ti (0.014) and Al. It has higher strength compare to the other 6000 series alloys. Alloy 6351 is a structural alloy which is available in plate form and commonly used for machining. Due to higher strength of 6351 has replaced 6061 alloy in various applications.

Thus, alloy such as 6351 have considerably more silicon than magnesium and other elements, silicon is formed  $Mg_2Si$  precipitate in 6351 alloy. The Al 6351 aluminum alloy is utilized in manufacturing sector because it has high strength, better bearing capacity, good weldability and workability. It is conjointly utilized in construction of boats, columns, chimney, rods, pipes, tubes, automobiles, bridges. Al (6351 H30) series alloy can be also utilized in structural and general engineering objects such as rail & road transport automobiles, bridges, cranes, roof trusses, rivets with a good surface finishing.

Si and Mg considered the main elements in 6xxx series, these elements are partially dissolved in  $\alpha$ -Al matrix and helps in formation in intermetallic phases depending on composition and solidification condition. In the technical 6xxx series aluminium alloys contents of Si and Mg are in the range of 0.5-1.2wt%, usually with a Si/Mg ratio more than one. In addition, the intentional metals like iron (Fe) and manganese (Mn) are always present.

Mg<sub>2</sub>Si ( $\beta$ ) phase increase the age hardening response of 6351 alloy. In Al-Mg-Si, Mn is used to improve the grain size. The different phases are formed in 6351 alloy such as AlFeSi, AlFeSiMn and  $\alpha$ -Al<sub>x</sub>(Fe,Mn)<sub>y</sub>Si<sub>z</sub> phase that helps in formation of Mg<sub>2</sub>Si crystals, which eventually affects the mechanical properties of alloys.

Al 6351 properties can be improved either by SPD (severe plastic deformation) and cryorolling. SPD technique is utilized in manufacturing sector and various commercial products. SPD produce ultrafine grains which increase both strength and ductility simultaneously. There are certain limitations of SPD technique such as high operational cost, difficulty to achieve long length product, higher strain rate and complicated processing of material.

Cryorolling is another technique to produce ultrafine grains and to overcome the limitation of SPD technique. Limited literature is available for Al 6351 alloy. So, present research is focused on development of ultrafine grained 6351 alloy using cryorolling.

## 1.2 LITERATURE REVIEW

**H. L. Stark et al (1988)** determined whether a crack be made to grow as a result of sustained unvarying applied stress when stress intensity value is less than that of critical stress intensity in an aluminium alloy 6351 T6. They found that stable crack growth occurred at stress intensities 50% of the critical stress intensity and in the absence of fatigue fluctuation of the stress intensity. And also suggest that the use critical stress intensity factor for the case sustained load design is not conservative unless adequate safety factor are used. There are various factors such as reduced size, shape and second phase hard particles are responsible to increases the sustained load fracture toughness.

**Sp. G. Pantelakis et al. (1995)** developed a fatigue crack growth retardation model (FCG) under approximation where yield stress varied along the path of crack growth when the material affected by an overload. And the analytical results correlated well with experimental data for 2024- T3 and 6061-T6 aluminium specimens. And found that deviations tend to extend with increasing crack length.

**J. W. H. Price et al. (1997)** developed a brand new approach for modelling sustained load cracking in aluminum gas cylinders that was used as self-contained underwater breathing device (SCUBA). And found a way of estimating constants within the crack growth equation by analysing unsuccessful cylinders and matching the theoretical model to the

observations and developed a brand new equation which offer a crack growth speed up to  $10^8$  quicker than earlier models.

**R. N. Ibrahim et al. (1998)** studied new thermomechanical technique which retard the fatigue crack growth (FCG) in aluminium alloy 6351 T6 and also improve apparent fracture toughness. And by application of thermomechanical conditioning cycle, the stress concentration factor reduced by 15% And life of aluminium gas cylinder increases.

**F. Bergner et al. (2004)** investigated the effect of microstructure on cyclic deformation behaviour of Al-Mg-Si aluminium alloy. And to studied this, they performed low cycle fatigue test on two aluminium alloy having different chemical compositions. And found that 6082 T6 shows cycle softening and hardening for axial rate below and above than 0.82% respectively. And also found that 6082 T6 shows ideal Masing behaviour while 6060 T6 shows stable cyclic behaviour. Non Masing behaviour is owing to particle /dislocation interaction.

**F. Bergner et al. (2004)** studied the dominant closure mechanism at constant- and variable-amplitude load for three different Al-Mg-Si aluminium alloys having different percentage of manganese (Mn) and chromium Cr. The alloy which contained higher percentage of Mn and Cr shows roughness induced closure mechanism because Mn/Cr dispersoid particles support planer slip mechanism and crack deflection resulting in decrease crack growth rates. Alloys having lower percentage of Mn and Cr shows plasticity induced closure mechanism. Roughness induced closure is the main-overload closure mechanism.

**L. P. Borrego et al. (2005)** studied the fatigue behaviour of thin Al-Mg-Si T6 due to a varied loading pattern having periodic single overload. They found that rate of retardation increase with overload periodicity and decrease with stress ratio increase. And also found decreasing load sequence level leads to higher crack growth retardation as compare to increasing one.

**Ran Guo v et al. (2008)** studied the fretting fatigue crack growth behaviour of riveted Al 6xxx components and determined the characteristics of crack initiation sites by means of experiments and numerical methods. And found that crack formation at the hole edge and minimal section delayed by increasing force and coefficient of friction. And above certain limit of fastening force, crack will initiate at  $45^0$  near the outer edge of the contact area. And fretting damage is affected by force and coefficient of friction.

**Yuri Estrin et al. (2009)** studied effect of severe plastic deformation (SPD) on fatigue behaviour of light alloys. SPD produced ultrafine grains and grain size reduced to micron and submicron scale. They found that tensile and fatigue strength increase sufficiently. And also found that the direct effect of solutes on fatigue strength is usually stronger than the grain refinement.

**M.V. Niranjan Reddy et al. (2014)** investigate the tensile behaviour of Aluminium alloy 6351 to the aerospace structure applications. They found that this alloy can be utilize an alternative material for aircraft design and also be used properly for pressure vessel application due to its superior corrosion resistance, good machinability properties.

**R. A. Gonglaves et al. (2015)** studied the effect of copper content on machinability of 6351 aluminium alloy. They found that we increase the percentage copper content in Al-Si-Mg-Cu aluminium alloy then hardness and ultimate tensile strength increase while percentage elongation decrease. It is due to stable hardening phases such as  $Al_5Cu_2Mg_8Si_6$  and  $Al_2Cu$ .

**Rajwinder Singh et al. (2015)** performed the crack growth analysis of rolled 6351 aluminium alloy using extended finite element methods. And found that 70 % RTR (room temperature rolled) Al alloy show greater crack growth resistance and larger plastic region as compare to 40 % RTR and bulk Al alloy. And also suggests that increments in properties, is mainly due to grain refinement.

**Kumar Gaurav et al. (2016)** studied the properties of aluminium alloy 6351 T6 using TIG welding. They suggest that hardness in HAZ and weld bead is higher as compare to base metal. Maximum harness and max impact energy was obtained at 100, 120 amps current and 5 lt/min gas flow rate. Improvement in property is due to small and fine size grains.

### 1.3 SCOPE OF WORK

From the literature available we can suggest that Al 6351 alloy is an important engineering material for various application. The property of Al 6351 alloy can be improved by forming and heat-treating at various temperature. So it is compulsory to study the mechanical and fatigue crack growth behavior of 6351 Al alloy. The following research work can be proposed on the basis of literature review for 6351 Al alloy.

- The effect of cryorolling and subsequent annealing on mechanical and microstructure behavior of Al 6351 alloy can be evaluated.
- Impact behavior of Al 6351 alloy can be investigated.

- Impact behavior of room temperature rolled and cryorolled Al 6351 alloy can be investigated.
- Fracture toughness of rolled and cryorolled Al 6351 alloy can be evaluated.
- Fatigue crack growth of rolled and cryorolled 6351 Al alloy can be investigated.
- Low and high cycle fatigue behavior of 6351 Al alloy can be evaluated.
- The effect of ageing treatment can be studied on the fracture and impact properties of 6351 Al alloy.

#### **1.4 OBJECTIVE OF CURRENT WORK**

On the basis of literature available in research proposal and from the scope of work following objective have been identified for M. Tech Dissertation work.

- To determine the mechanical properties of 6351 Al alloy through grain refinement using cryorolling.
- To study the effect of cryorolling on microstructure of 6351 Al alloy.
- To determine the Paris constants (C, m) of cryorolled 6351 Al alloy.
- To study fatigue and fracture behavior of cryorolled 6351 Al alloy and compare results with As- received alloy.

## 2.1 MATERIAL SELECTION

Material selection is the basic step in any design problem. The major objectives of any design are its functionality, manufacturability and all these parameters should be economically valid. Thus a proper choice of material depends on mechanical strength and cost of material. The Al 6351 alloy is usually used as extruded structures in road vehicles and railroad stock, tubing and pipe for carrying water, oil, or gasoline, infrastructure, transportation and aerospace due to its light weight, corrosion resistance and high strength to weight ratio, nontoxicity and good electrical conductivity. Chemical composition of this alloy is given in following **Table 2.1**.

**Table 2.1** Chemical composition of Al 6351 alloy

Elements	Si	Mg	Mn	Fe	Ti	Cu	Zn	Al
% weight	1.1	0.75	0.50	0.32	0.08	0.07	0.012	Rest

## 2.2 CRYOROLLING

We know that the properties of 6351 Al alloy can be improved by cryorolling. Cryorolling is the one simple plastic deformation process to obtain ultrafine grains. Cryorolling is preferred over SPD due to availability of setup. Rolling of metal at extremely low temperature i.e. cryogenic temperature suppresses the dynamic recovery which prompts to extreme strain hardening of metals like aluminum. Cryorolling is better alternative compared to other severe plastic deformation process due to (i) high stability (ii) low load requirement (iii) low cost (iv) simple procedure (v) capacity to produce long length products.

The Al 6351 alloy plate of thickness 30 mm was obtained from Mechanical department IIT Roorkee. This plate is cut into small-small pieces with dimensions 60 mm x 40 mm x 15 mm. after cutting, plates are heat treated at temperature of 540 °C for two hours and after that these pieces quenched into water. This process is called solution treatment (ST). Solution treated plate are ground by emery paper so that oxide film is removed. The solution treated Al plates (60 mm x 40 mm x 25 mm) are rolled at -196°C temperature to achieve 20 %, 40 %, 60 % and 80 % thickness reductions. To distribute the temperature uniformly thorough the plates, each solution treated samples are soaked in liquid nitrogen approximately 15 to



20 minutes for each rolling pass. In each pass thickness reduction is not more than 5 %. Hence many pass were given to obtain the desired result. The diameter and rolling speed of roll was 110 mm and 8 rpm respectively. The samples before cryorolling are shown in **Figure 2.1** and after cryorolling shown in **Figure 2.2**, respectively.

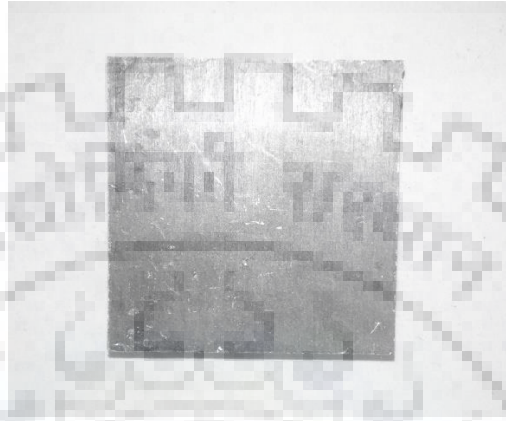


**Figure 2.1:** Sample of Al 6351 alloy before cryorolling



**Figure 2.2:** Sample of Al 6351 alloy after cryorolling.

### 2.2.1 Advantage of Cryorolling

- Cryorolling provide better strength as compare to cold rolling due to ultrafine grains.
- Handling of samples in cryorolling becomes easier than hot rolling.
- Less plastic straining is required in cryorolling to obtain ultrafine grains as compare to severe plastic deformation (SPD) techniques.
- Ductility of cryorolled sample improves by subsequent annealing.

### 2.2.2 Disadvantage of Cryorolling

- Cryorolling process is mainly suited for soft and ductile materials. It cannot be used for hard and brittle materials.

- Subsequent annealing is compulsory to improve ductility of cryorolled sample.

## **2.3 PURPOSE OF CRYOROLLING**

Cryorolling is done for various purpose which are given below.

### **2.3.1 Grain Size**

Cryorolling produce numerous ultrafine grains which causes increase in surface area of grain boundaries. Hence, this cause increase in numbers of overall barriers for the movement of dislocations, and greater force required for the dislocation movement to cross the barriers. Due to this reason strength of alloy increases.

### **2.2.3 Dislocation Density**

Cryorolling produced greater number of dislocations which piled up on the grain boundaries. Cryorolling increase dislocation density which improve strength but decrease the ductility.

### **2.2.4 Suppression of Dynamic Recovery**

Cryorolling results in suppression of dynamic recovery of aluminum alloy. The total internal energy of atoms decreases with decrease in temperature of the material. Therefore, the kinetic energy of atoms decreases which results in the suppression of dynamic recovery.

## **2.3 ROOM TEMPERATURE ROLLING**

Room temperature rolling performed at room temperature. Room temperature rolling is easy to perform as compare to cryorolling. But cryorolling produce ultrafine grains which improve mechanical and fatigue properties but room temperature rolling cannot develops ultrafine structure and improvement in mechanical and fatigue properties are lesser than that produce by cryorolling. So, cryorolling is chosen over room temperature rolling.

## **2.4 EXPERIMENTAL SET UP FOR CRYOROLLING**

The experimental set up for cryorolling is shown in **Figure 2.3**. The liquid nitrogen is utilized to achieve the required temperature to perform cryorolling operation of Al 6351 alloy. The liquid nitrogen plant is shown in **Figure 2.4**.



**Figure 2.3:** Cryorolling machine



**Figure 2.4:** Liquid nitrogen setup

The cryorolling include following apparatus.

- The rolling mill have two rollers of diameter ,110 mm. The rolling speed is set at 8 rpm so that friction loss among rollers and sample is reduced.
- A cryocan is used to store liquid nitrogen.
- A hot case (container) is used to hold the sample in liquid nitrogen.
- A digital Vernier is used for measuring thickness of different pieces.
- A lubricant (molybdenum disulfide) is used to reduce heat loss among rollers and samples.
- A set of gloves is used for handling of work piece.

## 2.5 CRYOROLLING PROCEDURE

Cryorolling process can be summarized in **Figure 2.5**. To get the desired result following points should be keep in mind.

- The rolling mill should be neat and clean. Proper lubricant is used to reduce heat loss.
  - The samples are soaked in liquid nitrogen approximately 15-30 minute before each pass. The time required for taking samples from container and placing it on milling mills must be very small.
  - The temperature of sample before and after cryorolling pass is found to be -160 °C and -70 °C respectively.
  - After each pass thickness of sample is measured with the help of digital Vernier.
  - More than 10 pass is required to achieve desired thickness reduction.
- Strain per pass ( $\epsilon$ )= $\ln$  [thickness after cryorolling/initial thickness before rolling]
- Cryorolling performed at very less strain rate i.e. 2 % so that rolling defects such as edge cracks and alligatoring defects can be avoided.

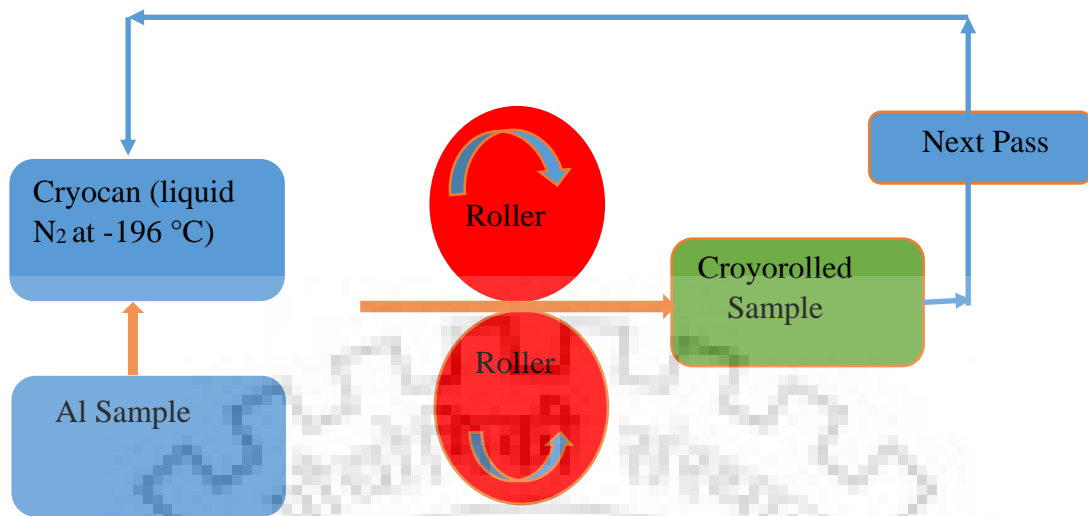


**Figure 2.5:** Cryorolling process

## 2.6 MICROSTRUCTURE CHARACTERIZATION

There are various schemes to characterize the microstructure of metals and alloys. The details of these schemes are given below.

### 2.6.1 Optical Microscopy

The microstructure of solution treated (ST) bulk alloy and cryorolled (CR) alloys is studied by LIECA DMI 5000 M optical microscope which is shown in following **Figure 2.6**. Following procedure is used in sample preparation. Small samples of dimensions 10 mm x 10 mm x 10 mm are cut from bulk alloy and cryorolled plates and these samples are mounted on sample holder to hold the samples properly. These samples are polished using silicon carbide water proof emery papers of 220, 400, 600, 800, 1000, 1200, 1500, 2000 and 3000 grit size. These samples are cloth polished with alumina powder of 3000 mesh size. Finally, samples are etched in poulton etchant and time for etching should be less than 30 second. The samples used for optical micrograph are shown in **Figure 2.6**. Optical micrographs are taken at different magnifications. And samples for optical micrograph are shown in **Figure 2.7**.



**Figure 2.6:** Optical microscope [8]



**Figure 2.7:** Optical micrograph samples

### 2.6.2 Field Emission Scanning Electron Microscope (FE-SEM)

The microstructure and EDAX analysis of solution treated and cryorolled are investigated using FE-SEM Quanta 200 FEG which is shown in figure **Figure2.8**.



**Figure 2.8:** FE-SEM QUANTA 200 FEG [9]

### 2.6.3 X-Ray Diffraction

X-ray diffraction is used to predict the different phases in the bulk and cryorolled alloys. X ray diffraction performed on all the samples using Cu,  $K\alpha$  radiation. The equipment Bruker AXS D8 XRD (**Figure 2.9**) is used for X-Ray diffraction.



**Figure 2.9:** XRD machine [10]

## 2.7 MECHANICAL TESTING PROCEDURE

Mechanical characterization procedure for bulk and cryorolled Al alloys are given below.

### 2.7.1 Tensile Testing

Tensile tests are used to predict and analyze the strength and ductility of bulk (ST), CR 20, CR 40, CR 60 and CR 80 Al alloy samples. The tensile samples are prepared in sub-size with axis parallel to rolling axis. The tensile specimen is made according to ASTM standard (E8/E8M-13a) having gauge length of 25 mm. The tensile specimens are cut with the aid of power Hacksaw (shown in **Figure 2.10**) and then machined into desired specification according to ASTM Standard. These samples are mechanically polished using silicon carbide emery papers of different grit sizes 220, 400, 600 to remove scratches, flaws and surface irregularities. Tensile tests are carried out on MTS 810 machine.

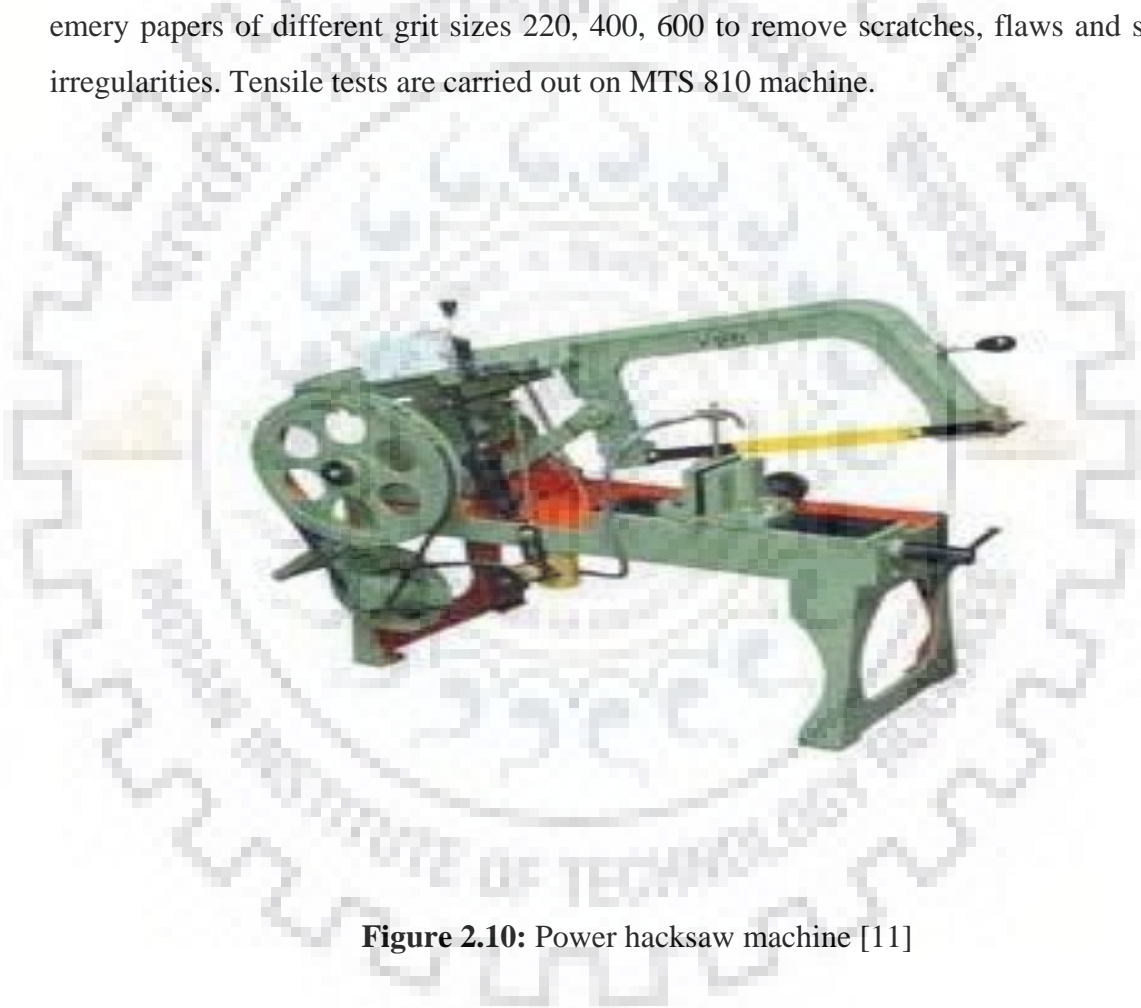


**Figure 2.10:** Power hacksaw machine [11]



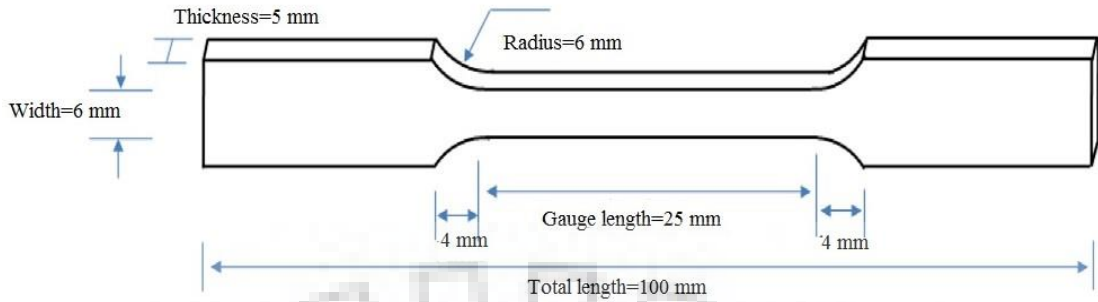


**Figure 2.11:** Geometry of tensile specimen [12]



**Figure 2. 12:** Tensile specimen

### 2.7.2 Hardness Testing

Hardness test is used to determine hardness and strength of the solution treated and cryorolled Al alloy samples. Hardness test is performed using automatic Mitutoyo micro-hardness tester having load capacity from 0.005 to 2000 gm. The hardness samples have dimensions (10 mm x 10 mm x 6mm) as per ASTM standard guideline. These samples are mechanically polished using silicon carbide emery papers of grit size 220, 400, 600, 800, 1000 and 1500 and finally cloth polished with alumina powder. The prepared hardness sample are shown in **Figure 2.10**. Vickers hardness test are performed according to ASTM (E384-16). All samples tested under a load 100 gm and time for loading is 15 seconds.

In Vickers harness tester, square base pyramid shaped diamond indenter is used and the face angle of indenter should be 136°. The Vickers hardness is calculated by the following formula.

$$H_v = \frac{2P \sin 68^\circ}{d^2} \text{ Kg/mm}^2$$

Where P=load (gram), d=diameter ( $\mu\text{m}$ )



**Figure 2. 13:** Micro hardness samples.



**Figure 2.14:** Mitutoyo hardness tester

### 2.7.3 Fatigue Crack Growth Testing

Fatigue Crack Growth (FCG) tests study are carried out for aluminium 6351 alloy. FCG tests is used to calculate the  $\Delta K_{Th}$  and Paris law constants. Compact Tension (CT) specimen is

used in FCG testing. The specimen is pre-cracked to introduce a sharp crack in the specimen. And the frequency and load ratio of pre-cracking are taken as 10 Hz and 0.1 respectively. The specimens are cut from bulk alloy and cryorolled alloy plates in L-T orientation as per ASTM E399 standard. And then compact tension (CT) type of specimens are prepared according to ASTM E 674-15. CT specimen shown in **Figure 2.16**.

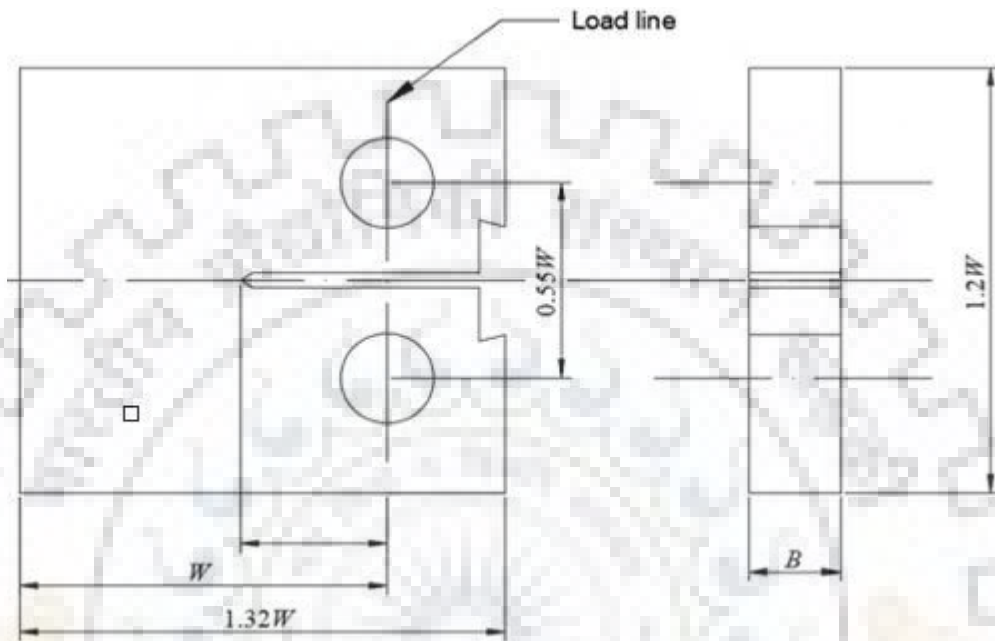


**Figure 2.15:** Geometry of compact specimen for FCG [13]



**Figure 2.16:** Compact Specimen for FCG

# MECHANICAL BEHAVIOR AND CHARACTERIZATION

---

### 3.1 INTRODUCTION

The performance of any component is dependent on its application and how and where it is utilized and the performance can be predicted by testing these components in laboratory. So mechanical behavior and characterization are used to calculate mechanical and various important properties. In this chapter mechanical behavior and characterization of bulk and cryorolled alloy are discussed in details. We know that mechanical properties of aluminium alloy can be increased by severe plastic deformation and cryorolling. Here, cryorolling is chosen for enhancing the properties of Al 6351 alloy.

### 3.2 MICROSTRUCTURE CHARACTERIZATION

Material properties dependent on microstructure and also microstructure characterization plays an important role in material science. Here some important technique like optical microscopy and FE-SEM are used for this purpose.

#### 3.2.1 Optical Microscopy

Samples of bulk and cryorolled Al alloy for optical microscopy are prepared as per ASTM standard and etched in modified Poulton's reagent having a mixture of 30 ml HCl, 40 ml HNO<sub>3</sub>, 2.5 ml HF, 12 gm CrO<sub>3</sub> and 42.5 ml H<sub>2</sub>O for less than 30 seconds. The microstructure of bulk and cryorolled alloy are examined using optical microscope. The optical micrograph for bulk (ST) alloy, CR 20, CR 40, CR 60 and CR 80 are shown in **Figure 2.16**. The optical micrograph of bulk shows lamellar grains which lying parallel to ingot axis and the micrograph of cryorolled 6351 alloy with 20 % reduction is not clear. But grains are elongated in the direction of rolling.

The grain size reduce is reduced to 960 nm and 650 nm for the cryorolled samples subjected to 60 % and 80 % reduction at cryogenic temperature. Cryorolling suppress the dynamic recovery and produce ultrafine grains.

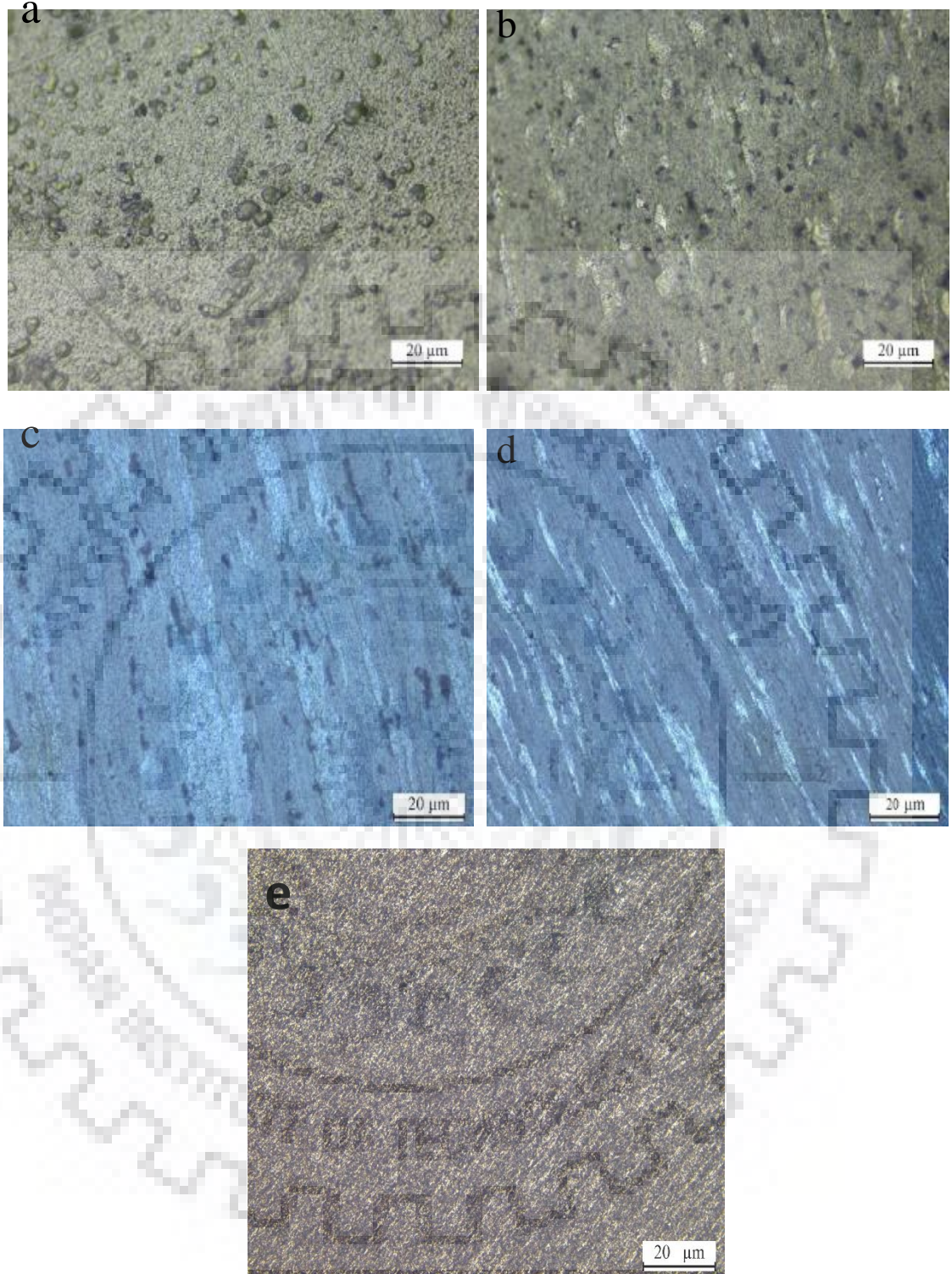


**Figure 3.1:** Optical micrograph of 6351 Al alloy (a) bulk alloy (b) 20 % CR (c) 40% CR (d) 60 % CR (e) 80 % CR

### 3.2.2 EDAX Analysis Using FE-SEM

EDAX (Energy dispersive X ray analysis) is used to detect presence and amount of chemical elements in the given samples. This technique based on the characteristic of x rays emitted by the atoms of the that element which is irradiated by a high energy beam. We know that each material and element has its own emitted X ray spectrum. EDAX spectrum of ST indicate the presence of insoluable  $\alpha$ -Al and  $\text{Al}_2\text{FeSi}$  phase along with  $\text{AlCuFeSi}$  phase. And presence of some dissolved phases.

While cryorolled samples indicates some dissolved Fe rich phase like  $\text{Al}_2\text{FeSi}$  and  $\text{AlCuFeSi}$ . And EDAX analysis also shows the precipitation of  $\text{Mg}_2\text{Si}$  metastable phases with different composition till the equilibruim phase  $\text{Mg}_2\text{Si}$  reached at grain boundaries. SEM image and EDAX analysis is shown on next page in **Figure 3.2 to 3.5**.



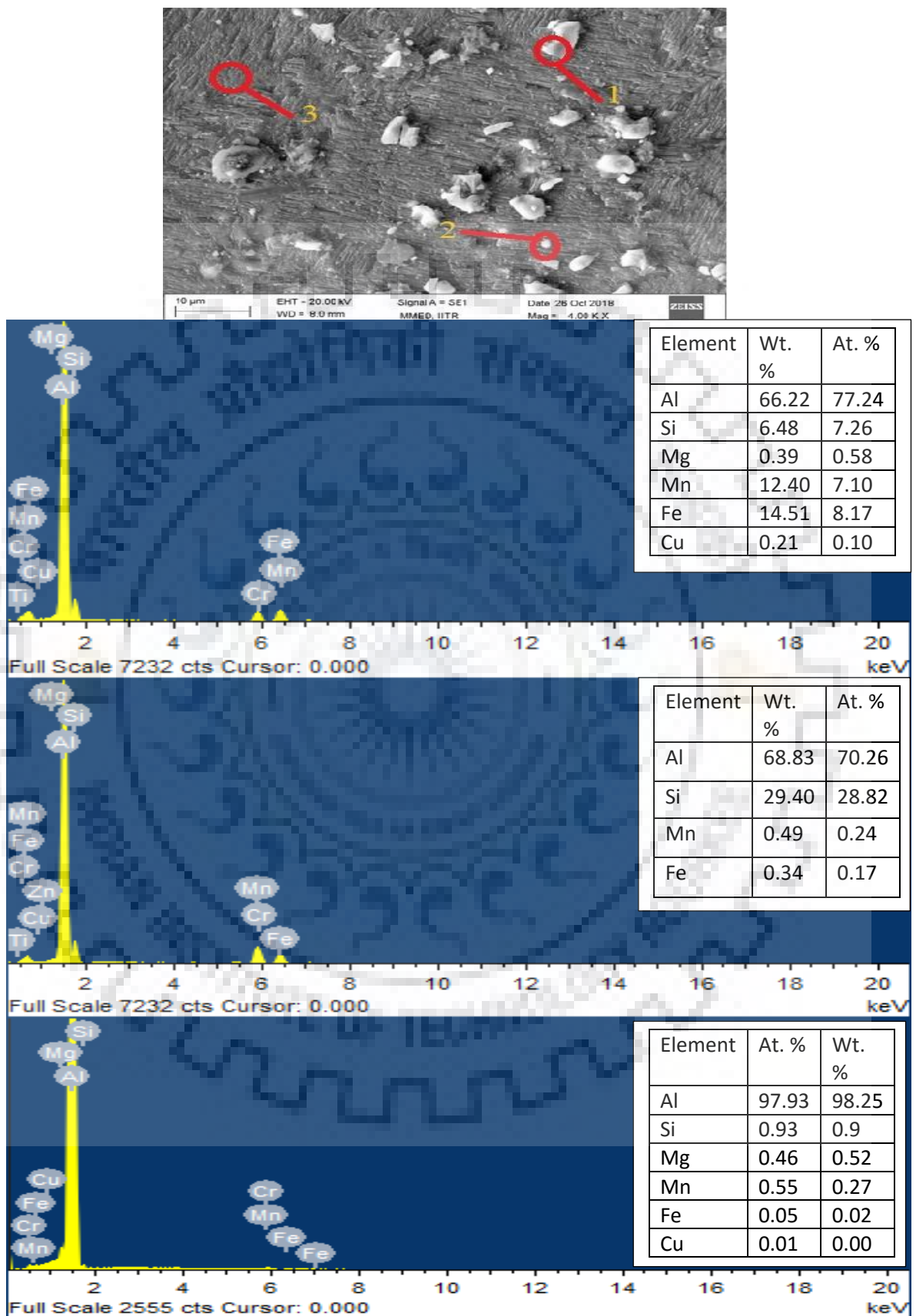
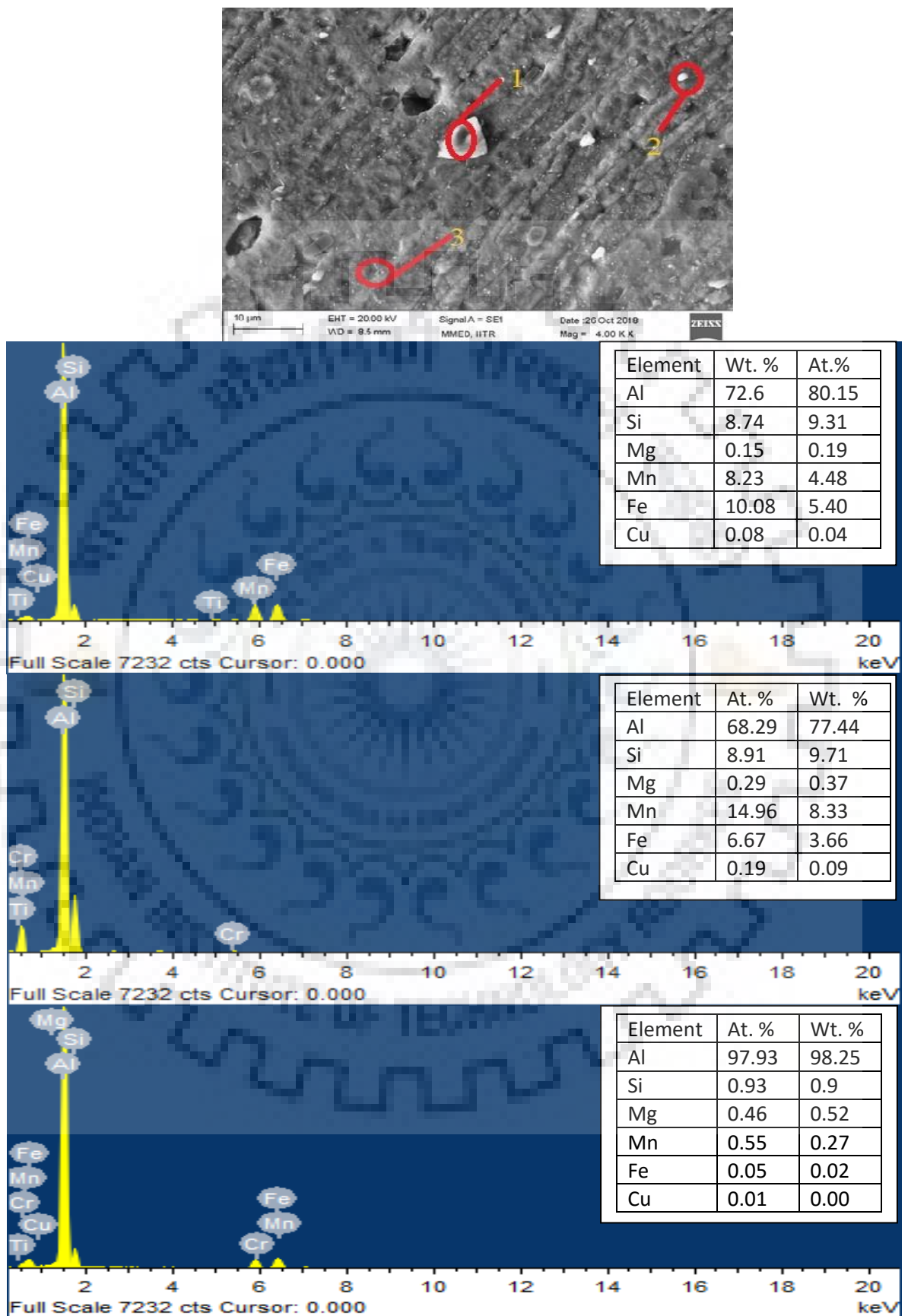
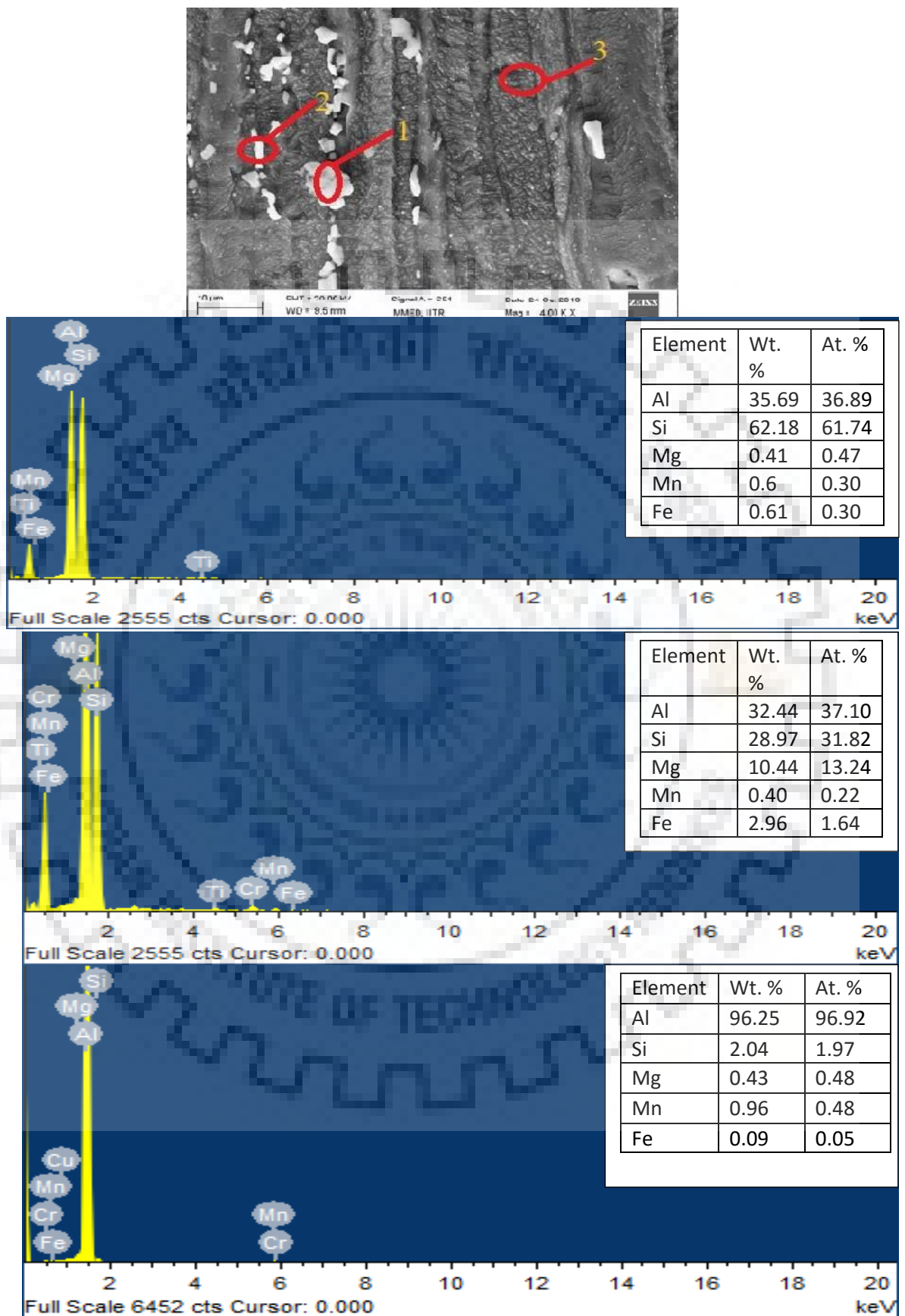


Figure 3.2: SEM micrograph with EDX analysis of ST Al 6351 alloy



**Figure 3.3:** SEM micrograph with EDX analysis of 20 % cryorolled 6351 alloy





**Figure 3.4:**SEM micrograph with EDX analysis of 40 % cryorolled 6351 alloy

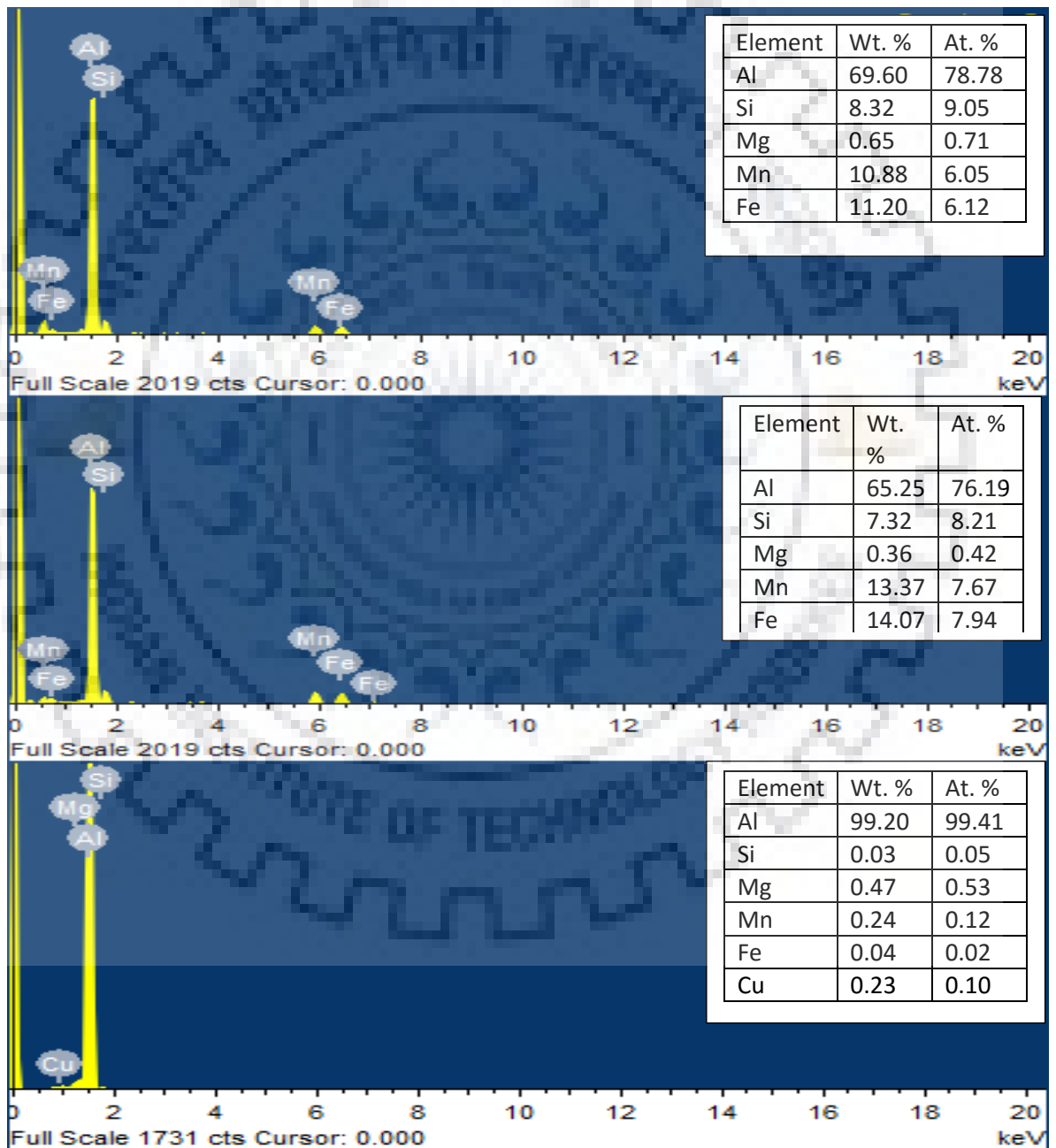
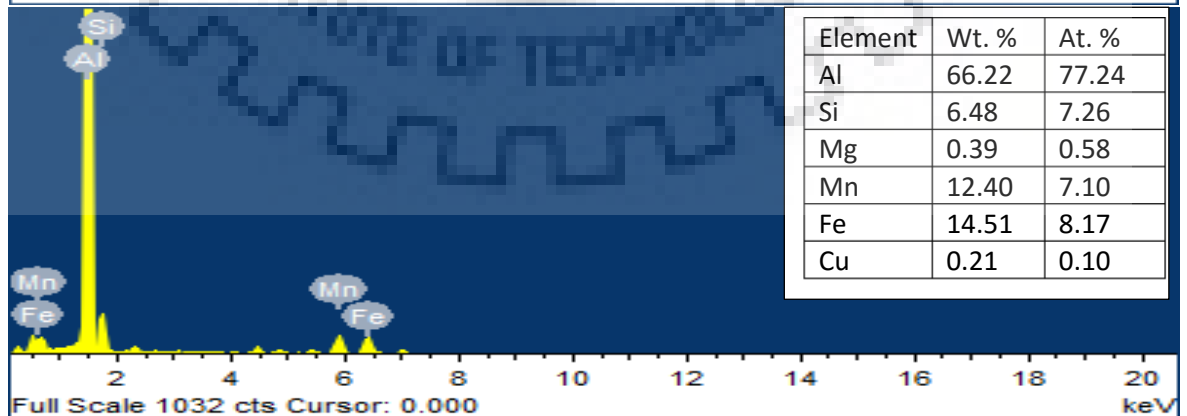
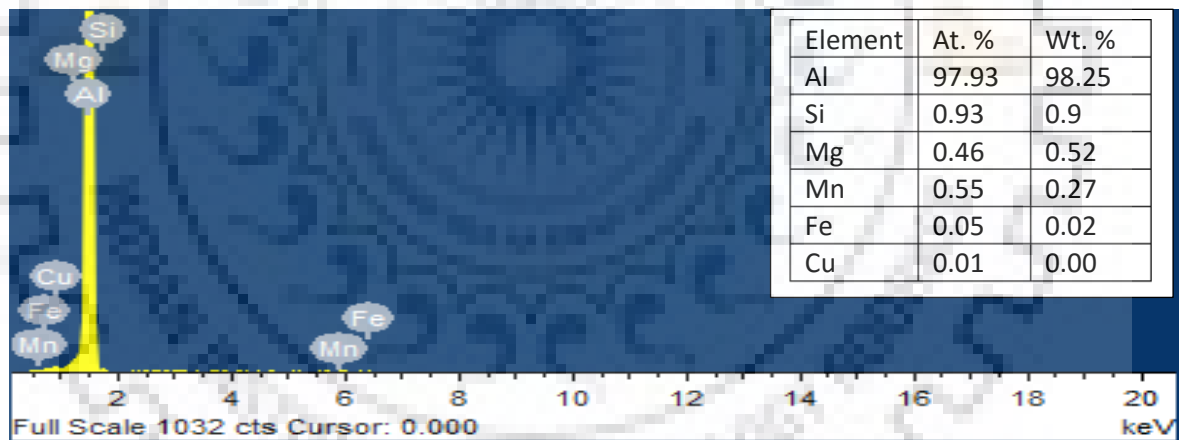
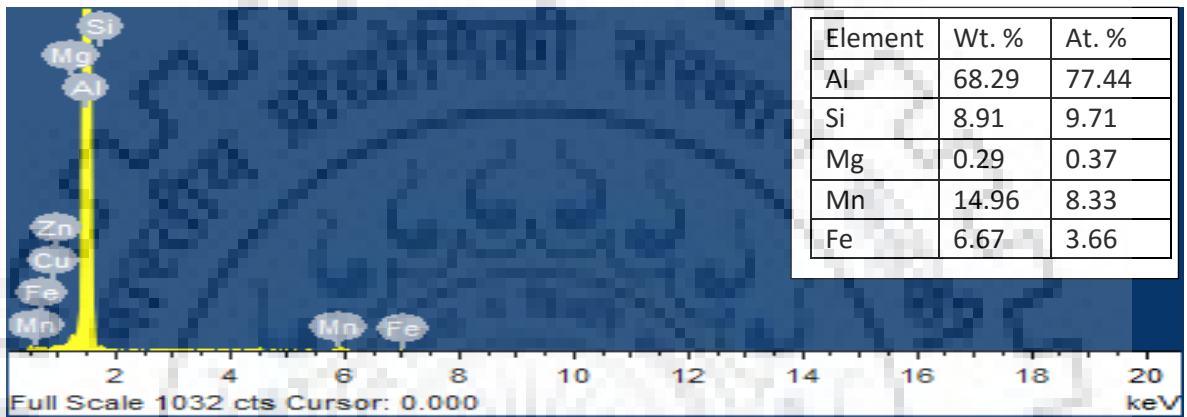
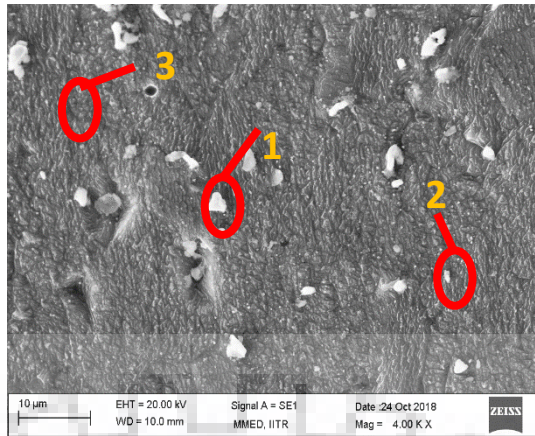


Figure 3.5: SEM micrograph with EDX analysis of 60 % cryorolled 6351 alloy



**Figure 3.6:** SEM micrograph with EDX analysis of 80 % CR cryorolled 6351 alloy

### 3.2.3 X Ray Diffraction Analysis

XRD analysis is used to determine crystal structure and phase present in the material. From the XRD pattern we can determine the following results.

- I. What crystal phases are in a mixture.
- II. Amount of each phase.
- III. Any amorphous material present in mixture.

The XRD pattern of 6351 Al alloy indicate the presence of  $Mg_2Si$  precipitates which is stable precipitates and formed at 2 theta angle of  $75.5^\circ$ . XRD pattern is shown in **Figure 2.22**.

XRD pattern shows different phases of  $Al_2FeSi$ ,  $Mg_2Si$  and  $AlCuMgSi$  are presents in bulk and cryorolled 6351 alloy. ST sample indicates presence of higher amount of  $Al_2FeSi$  and  $AlCuMgSi$  while increasing percentage of cryorolling,  $Al_2FeSi$  phase continuously decrease. And cryorolled samples also indicates presence of  $Mg_2Si$ .

Cryorolling causes suppression of dynamic recovery in the material and also increase dislocations density. High densities of dislocations provide site for nucleation of  $Mg_2Si$  phase.

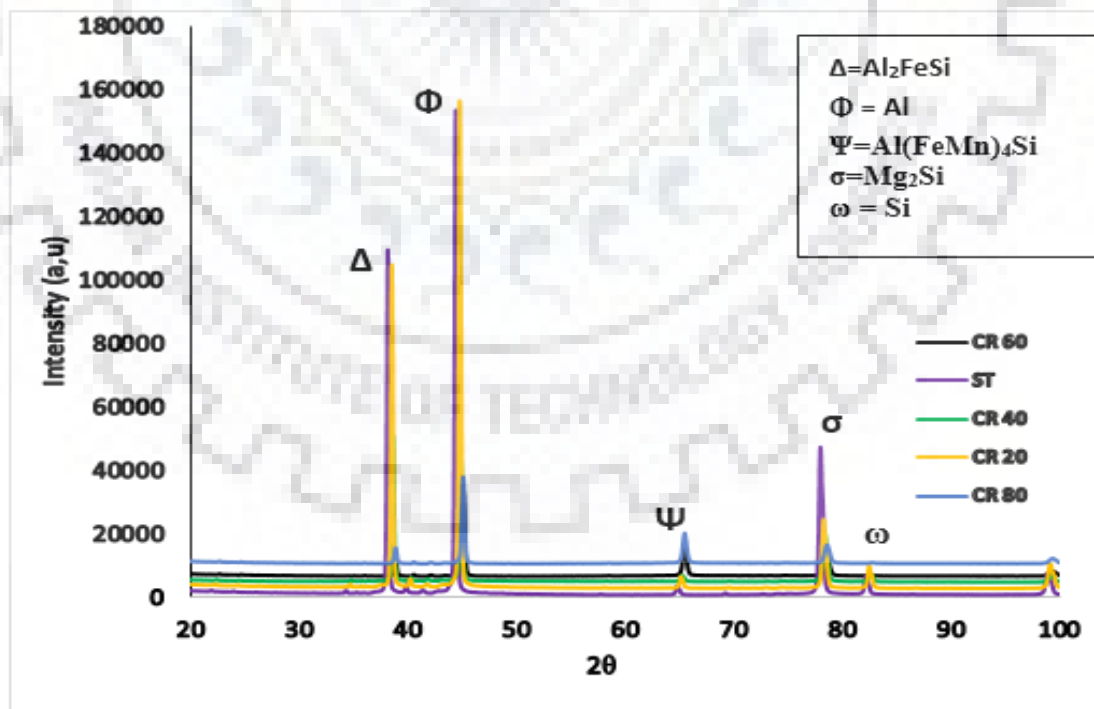


**Figure 3.7:** XRD analysis

### 3.3 MECHANICAL BEHAVIOR

Various tests like hardness test, impact test and tensile test are performed to investigate mechanical behavior of 6351 Al alloy.

#### 3.3.1 Tensile Test

Tensile test of bulk alloy, cryorolled alloy are done on MTS 800 machine. Three samples of each condition (bulk, CR 20, CR 40, CR 60 and CR 80) is tested to validate the result. % reduction in area, % elongation, yield strength and ultimate strength are calculated from tensile tests. These parameters are determined to discover optimum properties and compare the result with standard result. These parameters are calculated from formulas as given below.

Yield strength(YS)=0.2 % offset on stress-strain curve.

$$\text{Ultimate tensile strength (UTS)} = \frac{P_{max}}{A_0}$$

$$\% \text{ Elongation} = \frac{L_f - L_0}{L_0} \times 100$$

$$\% \text{ Reduction} = \frac{A_0 - A_f}{A_0} \times 100$$

Where  $P_{max}$ =maximum load

$L_f$  = Final gauge length

$L_i$  = Initial gauge length

$A_0$  = Initial cross area

$A_f$  = Final cross section area

The yield strength and ultimate tensile strength (YS, UTS) of bulk (ST), cryorolled 6351 alloy with 20 % reduction (CR 20), 40 % reduction (CR 40), 60 % reduction (CR 60) and 80 % reduction (CR 80) found to be (140 MPa, 202 MPa), (230 MPa, 262 MPa), (260 MPa, 332 MPa), (300 MPa, 368) and (340 MP, 415 MPa) respectively. The YS and UTS of CR 20 increase 64 % and 30 % as compare to ST alloy. And YS of CR40 CR 60 and CR 80 increased by 114 %, 137 % and 150 % while YTS increased 64 %, 80% and 105 % as compare to ST 6351 alloy. However, ductility of different samples such as ST, CR 20, CR 40, CR 60 and CR 80 observe to be 20 %, 12 %, 10 %, 7 % and 4 %. Here strength is increased while ductility decrease. So we need to optimise the properties so that strength and

ductility can be increased simultaneously through aging process. Stress vs plastic strain curve for cryorolled Al alloy 6351 is shown in **Figure 3. 8.**

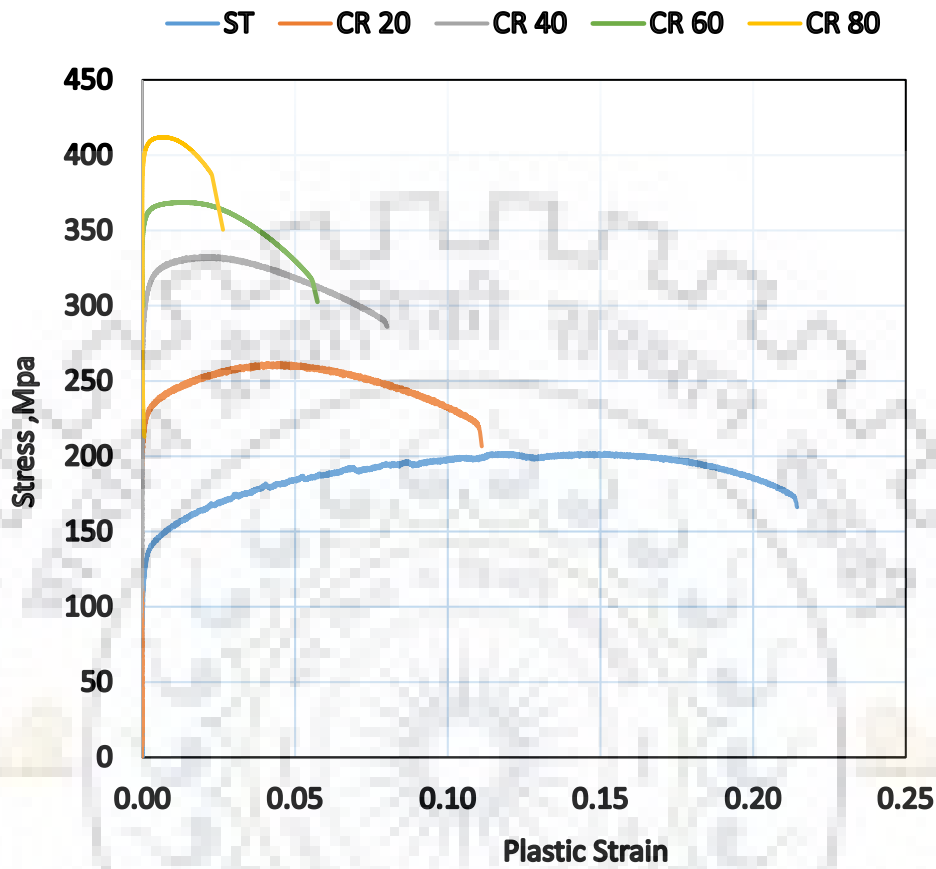


**Figure 3.8:** Engineering stress vs Plastic Strain Plot at room temperature

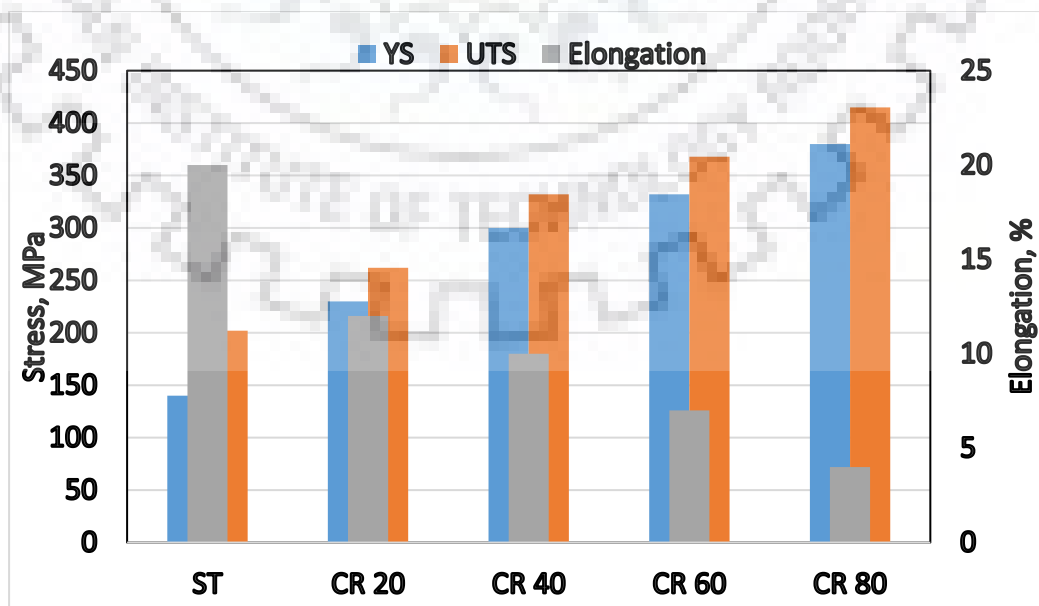


**Figure 3.9:** UTS, US and Elongation of ST, CR 20, CR 40 and CR 60 Al alloy 6351.

**Table 3. 1:** Ultimate strength (UTS) and Yield strength (YS) and % Elongation at room temperature for Al 6351 alloy

AT RT	YS (MPA)	UTS (MPA)	% EL
ST	140	202	20
CR 20	230	262	12
CR 40	260	332	10
CR 60	300	368	7
CR 80	340	415	4

### 3.3.2 Micro Hardness Testing.

Hardness of bulk and cryorolled samples are determined. Hardness value of cryorolled samples differs from solution treated samples. This shows that cryorolling increase the strength as well as hardness of the material. This change in hardness value is due to change in microstructure of cryorolled samples. Hardness value of ST, CR 20, CR 40, CR 60 and CR 80 is shown in **Figure 3.8**. The hardness of the cryorolled samples with 20 % thickness reduction, 40 % reduction, 60 % reduction and 80 % reduction is found to be 80 Hv, 110 Hv, 130 Hv and 150 Hv. The hardness of cryorolled samples increase due to increments in dislocation density and arrangement of ultrafine grains which is produced by severe plastic deformation. The reason for increasing hardness can be explained by mechanism of dynamic recovery which was suppressed during cryorolling and produce ultrafine grains. cryorolling produced ultrafine grains i.e. average size of grains decrease. This is explained by the Hall-Petch relation. According to this relation, yield strength is inversely proportional to root square of grain diameter i.e. smaller grain diameter higher the strength of the material. Also more and more grain boundaries are produced due to cryorolling. These grain boundaries restrict the movement of dislocation which pile up at grain boundaries which results increase in strength.

As we seen that cryorolling increase the strength but reduce ductility so to optimise the hardness of 6351 alloy aging is done at various temperature and for different time limit. **Tables 3.2, 3.3 and 3.4** show the hardness value of 6351 alloy at temperature of 100°C, 148°C and 180°C for different time limit 3h, 6h, 9h, 12h, 20h and 48h. The maximum value of hardness is obtained at temperature of 100°C and 12h for different case (CR 20, CR 40, CR 60 and CR 80). After aging fine precipitate is formed inside the grains therefore, hardness

increase. After aging treatment the optimum hardness value of cryorolled samples (CR 20, CR 40, CR 60 and CR 80) are found to be 90 Hv, 120 Hv, 145 Hv and 170 Hv.

**Table 3.2:**Hardness for Al 6351 alloy at room temperature

<b>S.NO.</b>	<b>Forms of Alloy</b>	<b>Vickers Hardness (HV)</b>
<b>1</b>	<b>Bulk</b>	<b>67</b>
<b>2</b>	<b>CR 20</b>	<b>80</b>
<b>3</b>	<b>CR 40</b>	<b>110</b>
<b>4</b>	<b>CR 60</b>	<b>130</b>
<b>5</b>	<b>CR80</b>	<b>150</b>

**Table 3.3:**Hardness and Aging time for 20 % CR Al 6351 alloy

<b>S.N.</b>	<b>Aging time (hrs)</b>	<b>Hardness (MPa)</b>		
		<b>100°C</b>	<b>148°C</b>	<b>180°C</b>
<b>1</b>	<b>3</b>	<b>82</b>	<b>70</b>	<b>75</b>
<b>2</b>	<b>6</b>	<b>85</b>	<b>75</b>	<b>73</b>
<b>3</b>	<b>9</b>	<b>86</b>	<b>82</b>	<b>72</b>
<b>4</b>	<b>12</b>	<b>90</b>	<b>85</b>	<b>70</b>
<b>5</b>	<b>20</b>	<b>75</b>	<b>73</b>	<b>62</b>
<b>6</b>	<b>48</b>	<b>70</b>	<b>70</b>	<b>65</b>

**Table 3.4:**Hardness and Aging time for 40 % CR Al 6351 alloy

<b>S.N.</b>	<b>Aging time (hrs)</b>	<b>Hardness (MPa)</b>		
		<b>100°C</b>	<b>148°C</b>	<b>180°C</b>
<b>1</b>	<b>3</b>	<b>111</b>	<b>115</b>	<b>120</b>
<b>2</b>	<b>6</b>	<b>110</b>	<b>110</b>	<b>110</b>
<b>3</b>	<b>9</b>	<b>115</b>	<b>115</b>	<b>100</b>
<b>4</b>	<b>12</b>	<b>120</b>	<b>120</b>	<b>95</b>
<b>5</b>	<b>20</b>	<b>110</b>	<b>100</b>	<b>85</b>
<b>6</b>	<b>48</b>	<b>100</b>	<b>95</b>	<b>70</b>



**Table 3.5:**Hardness and Aging time for 60 % CR Al 6351 alloy

S.N.	Aging time (hrs)	Hardness (MPa)		
		100°C	148°C	180°C
1	3	132	135	140
2	6	135	140	135
3	9	137	135	130
4	12	145	140	120
5	20	137	135	110
6	48	130	125	105

**Table 3.6:**Hardness and Aging time for 80 % CR Al 6351 alloy

S.N.	Aging time (hrs)	Hardness (MPa)		
		100°C	148°C	180°C
1	3	152	150	155
2	6	155	152	145
3	9	160	155	150
4	12	170	160	140
5	20	150	145	130
6	48	140	130	110

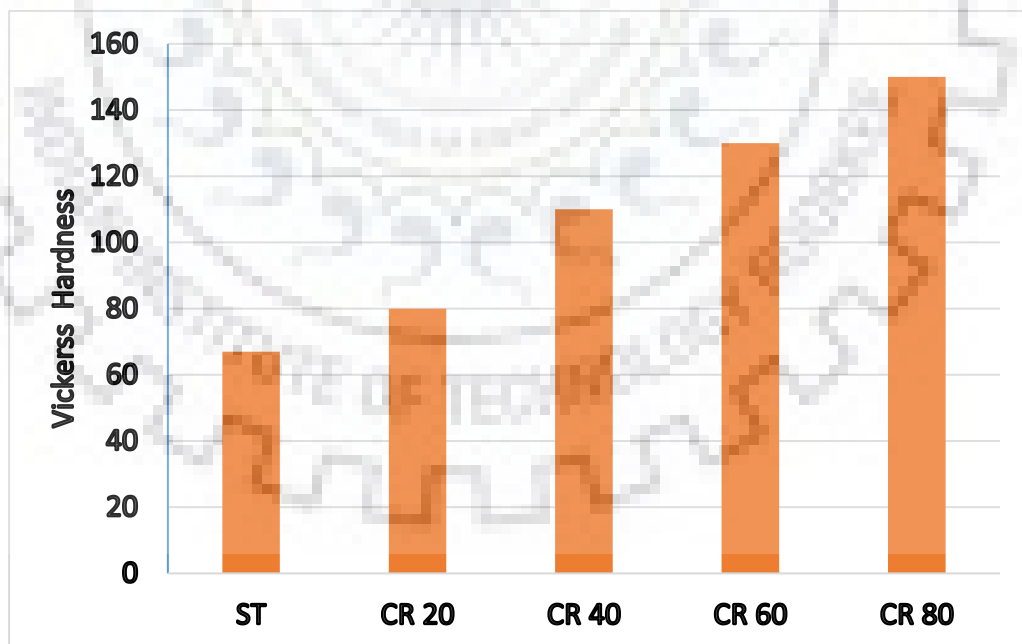


**Figure 3.10:** The hardness value of ST, CR 20, CR 40, CR 60 and CR 80 Al alloy 6351 at room temperature.

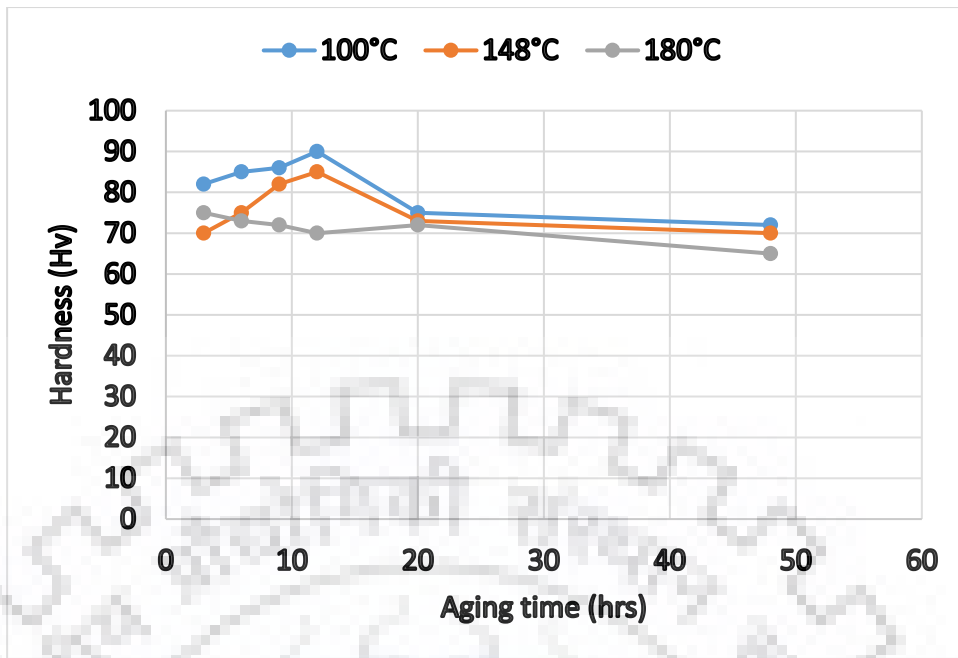


**Figure 3.11:** The variation of hardness value of 20 % CR Al alloy 6351 with temperature and aging time

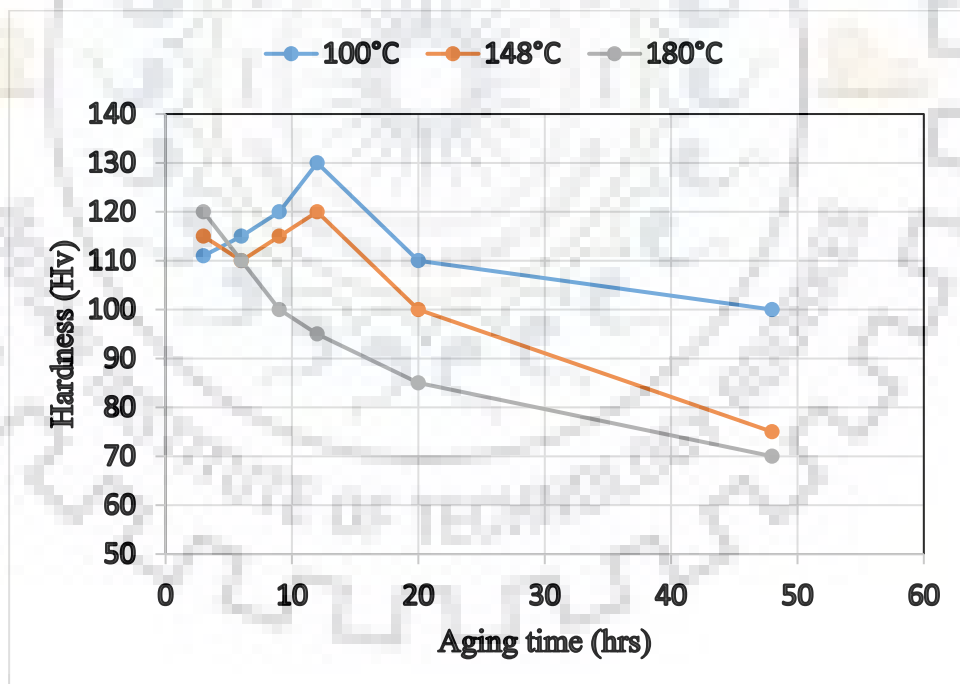


**Figure 3.12:** The variation of hardness value of 40 % CR Al alloy 6351 with temperature and aging time

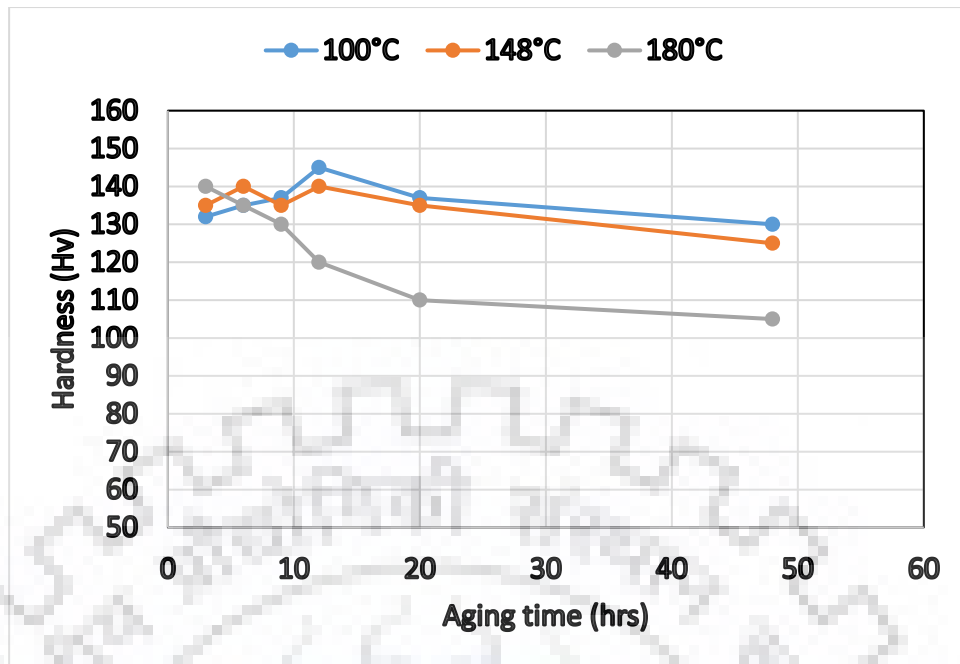


**Figure 3.13:** The variation of hardness value of 60 % CR Al alloy 6351 with temperature and aging time

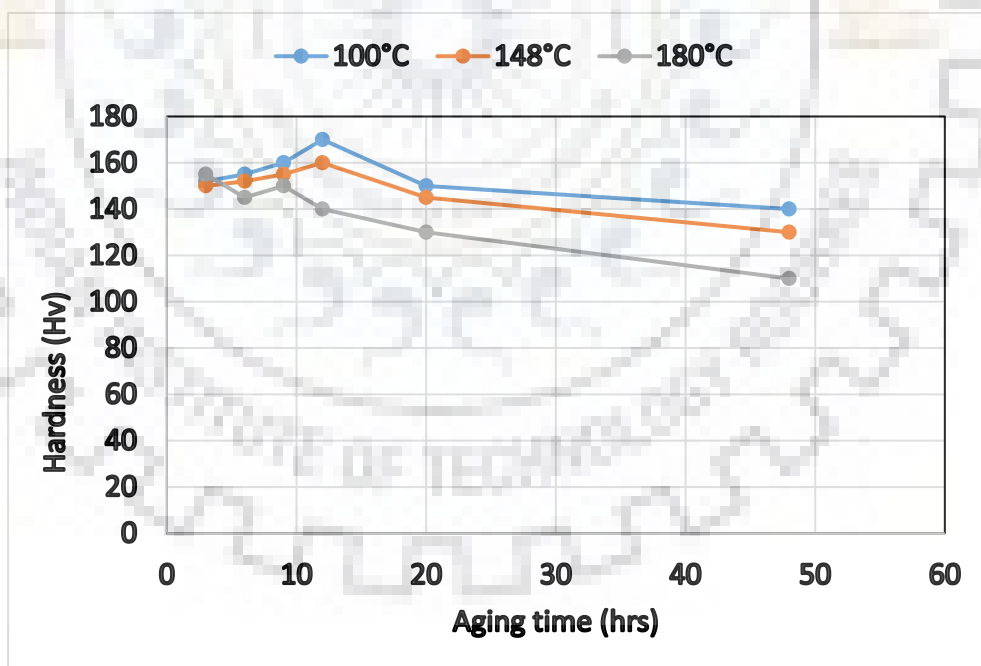


**Figure 3.14:** The variation of hardness value of 80 % CR Al alloy 6351 with temperature and aging time

### 3.3.3 Effect of Aging on Mechanical Properties.

After cryorolling mechanical properties like strength, hardness increase, simultaneously ductility decrease. So to optimize the strength and ductility aging is done at different temperatures for different aging time. We consider four different cases which are 20%, 40 % CR, 60% CR and 80% CR. Aging time is determined from literature presented in different research papers.

The effect of aging on stress-strain behavior of cryorolled aluminum alloy 6351 for different thickness reduction is described here. we have taken 3 different cases (40 % CR, 60 % CR and 80 % CR). The yield stress and ultimate stress increase with aging for these cases and given in **Tables 3.7, 3.8 and 3.9**. The flow stress increase due to suppression of dynamic recovery. However, overaging decrease the strength and hardness, it is due to precipitation growth. Stress strain curve for 40 % CR, 60 % CR and 80 % CR shown in Fig at different temperature 100°C, 125°C, 148°C and 180°C respectively. For 40 % CR, 60 % CR and 80 % CR yield and ultimate strength increase at temperature 100°C for 12 hours. Aging times for each case are chosen 12 h, 20 h and 30 h at 100°C, 68 h at 125°C, 20 h, 30 h at 148°C and 6 h, 12 h at 180°C respectively. From experiment we found that optimum mechanical properties obtained at temperature 100°C for 12 hours for each case. The yield strength of CR 40 increase from 260 MPa to 280 MPa and ultimate strength increase from 332 MPa to 358 MPa and also ductility also increases from 10 % to 12 %. Similarly, for CR 60 and CR 80 YS increase from 300 MPa to 320 MPa and 340 MPa to 365 MPa respectively. And UTS increase from 368 MPa to 389 MPa, 395 MPa to 415 MPa respectively. And ductility of CR 60 and CR 80 increase from 7 % to 9 % and 4 % to 6 % respectively.

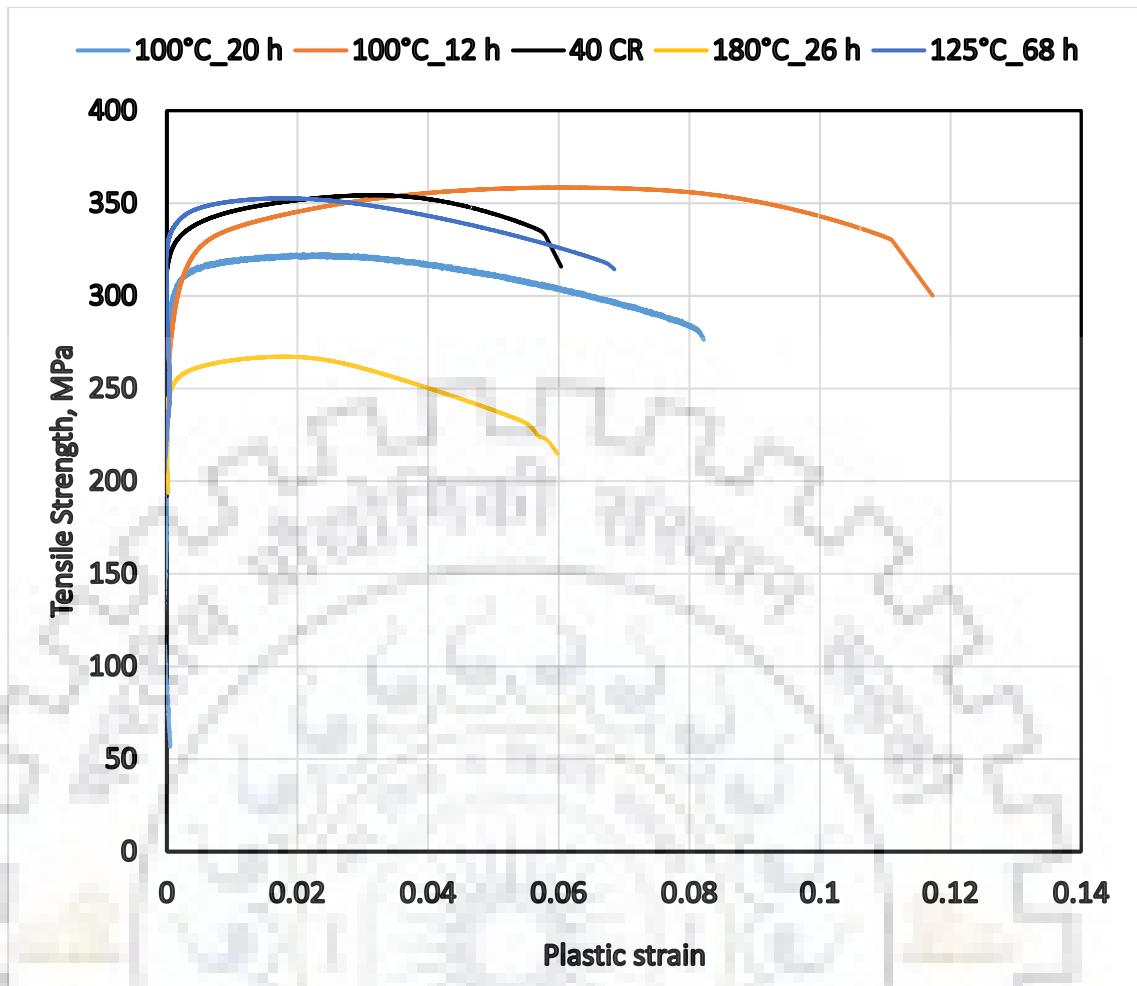


**Figure 3.15:** Stress vs plastic strain curve of 40 % CR 6351 alloy at various temperature and aging time.

**Table 3.7:** Yield strength, Ultimate strength and Aging time for 40 % CR Al 6351

S.N.	Aging temp (T°C)	Aging time (hrs)	YS (MPa)	UTS (MPa)
1	40 CR	0	270	332
2	100°C	12	280	358
3	125°C	68	250	354
4	148°C	20	230	316
5	180°C	6	200	267

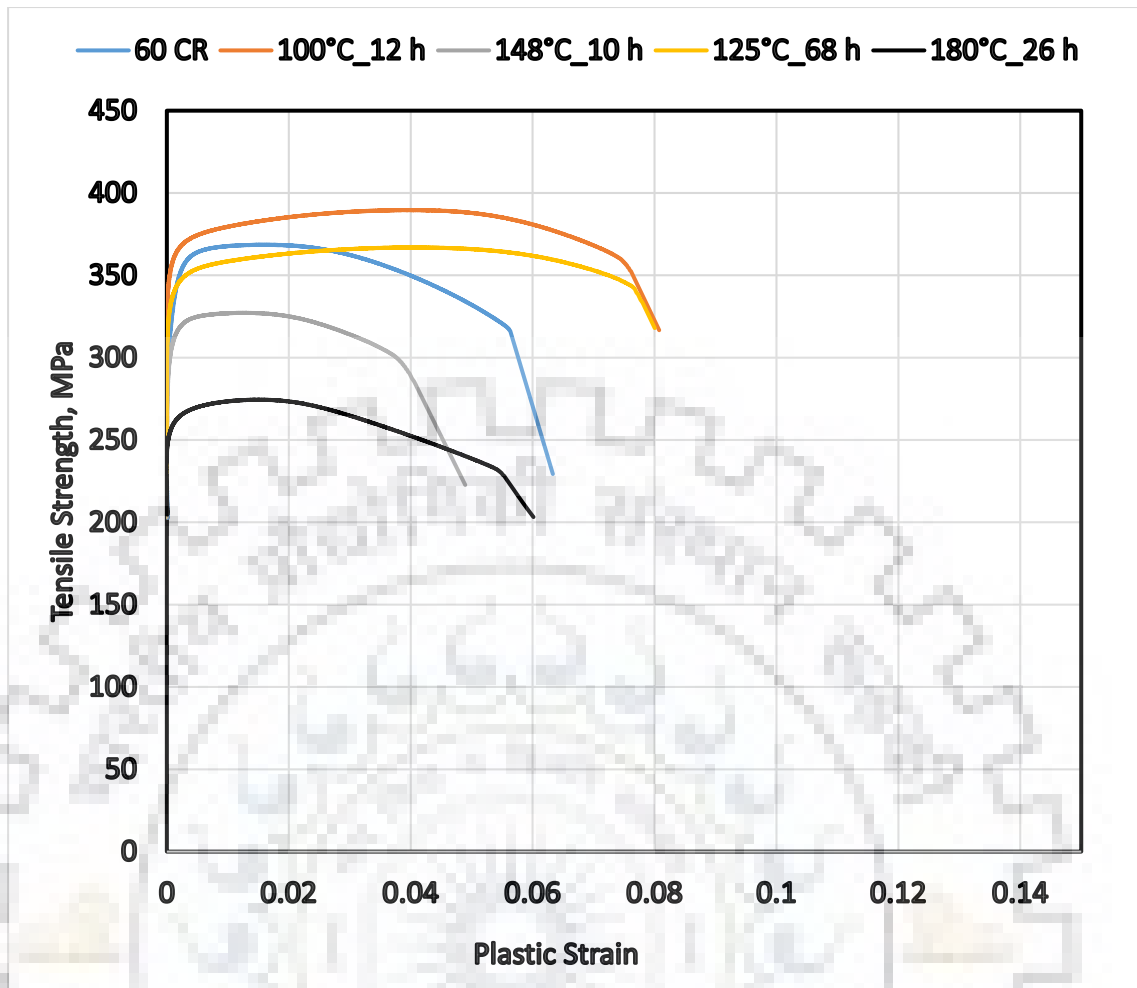


**Figure 3.16:** Stress vs plastic strain curve of 60 % CR 6351 alloy at various temperature and aging time

**Table 3.8:** Yield strength, Ultimate strength and Aging time for 60 % CR Al 6351 alloy.

S.N.	Aging temp (T°C)	Aging time (hrs)	YS (MPa)	UTS (MPa)
1	60CR	0	310	368
2	100°C	12	320	389
3	125°C	68	280	366
4	148°C	20	250	327
5	180°C	6	200	274

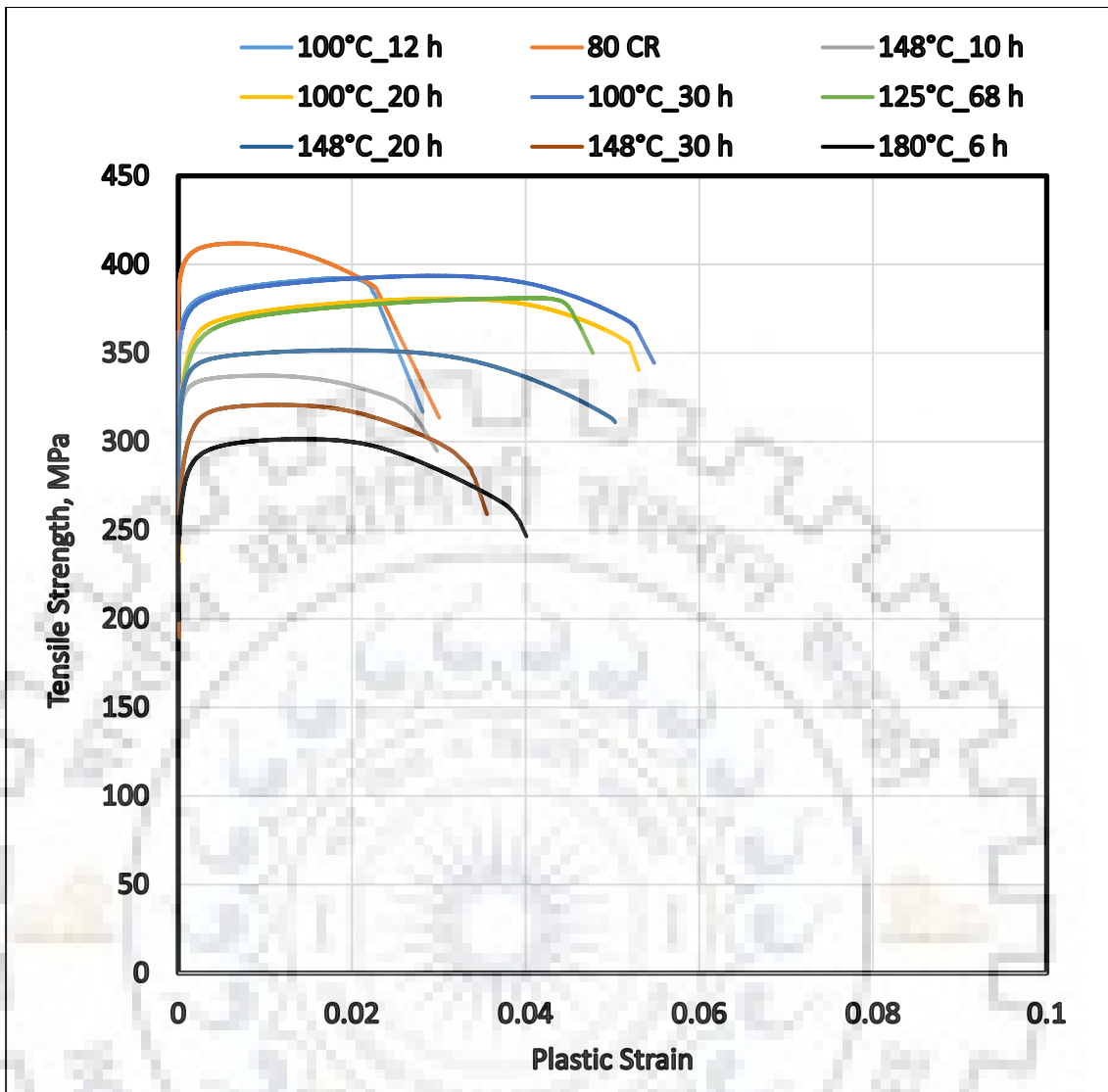


**Figure 3.17:** Stress vs plastic strain curve of 80 % CR 6351 alloy at various temperature and aging time.

**Table 3. 9:**Yield strength, Ultimate strength and Aging time for 80 % CR Al 6351 alloy.

S.N.	Aging temp (T°C)	Aging time (hrs)	YS (MPa)	UTS (MPa)
1	80 CR	0	340	395
2	100°C	12	365	415
3	100°C	20	310	380
4	100°C	30	304	393
5	125°C	68	286	381
6	148°C	20	272	351
7	148°C	30	294	320
8	180°C	6	241	300
9	180°C	12	220	278

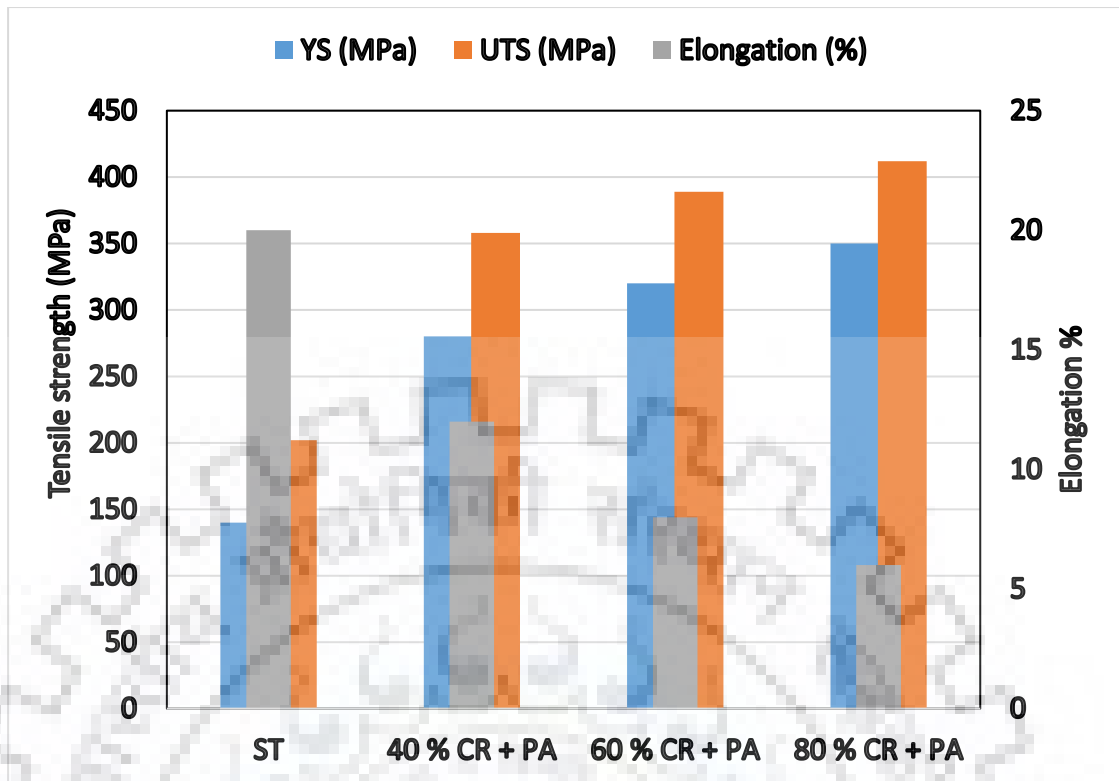


**Figure 3.18:** Optimum properties (YS, UTS and Elongation) of 6351 Al alloy for different thickness reduction.

### 3.4 Fractography

Fractography is used to examine the fracture surface and also to find out the cause to surface failure.

#### 3.4.1 Tensile Surface Fractography

Tensile test usually performed to determine the strength of Al 6351 alloy. The strain rate is taken  $5 \times 10^{-4}$  depending on application of Al alloy 6351. To examine the fracture surface of tensile specimen Fe-Sem is used. Fractograph of tensile test for ST, 20 % CR, 40 % CR, 60 % CR and 80 % CR are shown in **Figure 3.19**. ST Al alloy fractograph shows bigger size of dimples and less number of voids that cause the material fails in ductile manner. While cryorolled samples like 20 % CR, 40 % CR, 60 % CR and 80 % CR shows well defined fine dimples on fracture surface which mean that if we increase cryorolling than material fails approximately in brittle manner as shown in case of 80 % CR case. As the increase the reduction in thickness through cryorolling, the dimples size is decrease. And dimples size found to be  $1 \mu\text{m}$  for 80 % CR Al 6351 alloy.



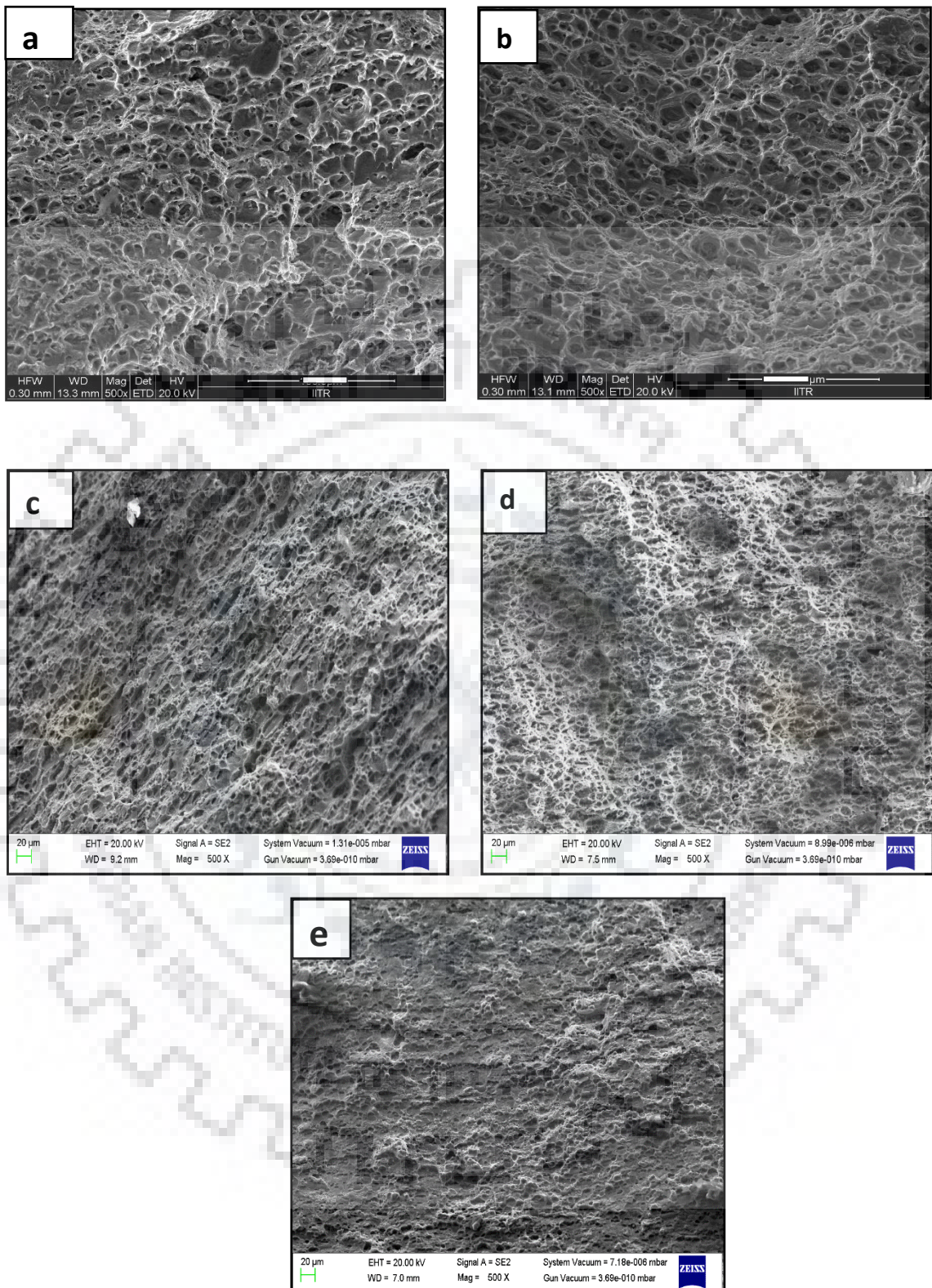


**Figure 3.19:** Tensile fractographs of (a) ST (b) 20 % CR (c) 40 % CR (d) 60 % CR (e) 80 % CR Al 6351 alloy.

## FATIGUE CRACK GROWTH BEHAVIOR

### 4.1 INTRODUCTION

Various studies show that between 50 to 90 percent of all mechanical failures are due to fatigue failures. Fatigue failures cause due to repeated loading and occurs at a stress much below the ultimate strength of the material and often below the yield strength. Fatigue failure can be seen any field from simple components such as door spring, electric light bulb to complex structure like aircraft, ships, road vehicles. Fatigue life can be calculated from S-N curve. But there are certain limitations with S-N curve. S-N curve does not predict accurate fatigue life of material. It does not explore the mechanism of failure and has a large scatter. And fatigue data generated for small component cannot be applicable for large components

So, for better understanding of failure mechanism crack initiation and crack growth both are considered together. Crack initiation might be occurred at the tip of an existing crack or at some point of a free surface. A fatigue crack grows with each applied load cycle. Initially crack growth per unit cycle is extremely low. But as the crack grows, it becomes quite large and crack is about to become critical then failure occurs.

Fatigue crack growth is divided into three regions (i) crack nucleation (ii) stable crack growth (iii) unstable crack growth or sudden failure. Fatigue crack growth curve is shown in **Figure 4.1**

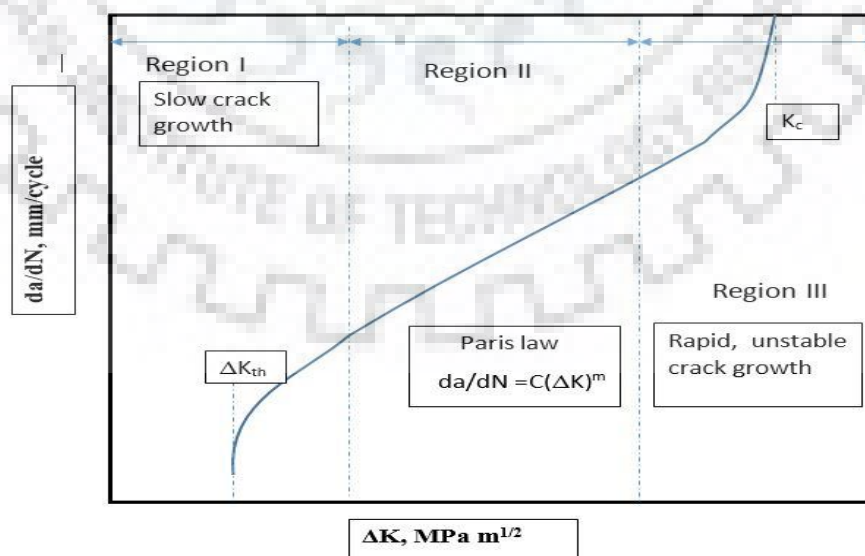


**Figure 4.1:** Fatigue crack growth curve [14]

## 4.2 FATIGUE CRACK GROWTH (FCG)

Fatigue crack growth generally refers to the second stage of fatigue life which is stable crack propagation. FCG deals with the number of cycles required to grow a crack from initial to critical size of crack. A crack length versus cycles curve is shown in **Figure 4.2** which represents fatigue and useful life of a cracked component.

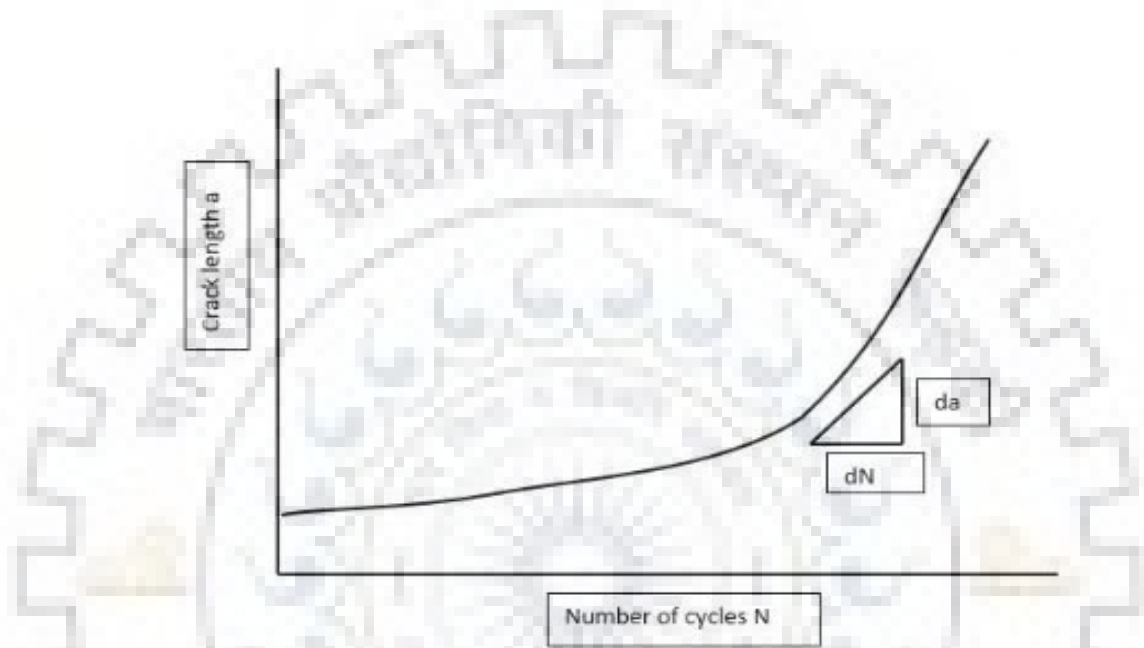


**Figure 4.2:** Crack length versus cycles curve [15]

To study the FCG behavior various law are given and FCG depends on  $\Delta K$  and stress ratio  $R$ .

$$\frac{da}{dN} = C(\Delta K, R)$$

But in case of 2<sup>nd</sup> region of curve, the FCG mainly depends on  $\Delta K$  but not on stress ratio Paris law is the most popular fatigue crack growth model in material science and fracture mechanics and given by

$$\frac{da}{dN} = C(\Delta K)^m$$

Where  $da/dN$  is the crack growth rate,  $a$  is crack length,  $C$  and  $m$  are constant that depend on material, stress ratio and environment. And  $\Delta K$  is the range of stress intensity factor.

$$\Delta K = K_{max} - K_{min}$$

the objective of this test to determine  $\Delta K_{th}$  and Paris constants. different type of specimen used for FCG test such as compact tension (CT), the middle tension (MT) specimen. CT specimen used to study FCG behavior of 6351 al alloy.

### 4.3 FCG TEST PROCEDURE

FCG test performed as per ASTM E647-15 standard to find out  $\Delta K_{th}$  and Paris law constant. According to ASTM E647-15 fatigue crack growth can be carried out by three methods which are given below.

1. K increasing
2. K decreasing
3. Constant load test

#### 4.3.1 Fatigue Pre-cracking

The purpose of pre-cracking is to introduce cracks with a minimum crack-tip radius. The final  $K_{max}$  should be 40 to 50 % less than initial  $K_{max}$  of material. For FCG the final  $K_{max}$  during pre-cracking should be within 5% range and  $K_{max}$  should be as low as possible. Fatigue pre-cracking should not less be less than 0.10B, h, or 1.0 mm, whichever is greater.

#### 4.3.2 K decreasing

This test is performed when crack growth rate is below  $10^{-8}$  m/cycle. The test may then be continued at constant force limits to obtain comparison data under K-increasing conditions. The K-decreasing test is not recommended at fatigue crack growth rates above  $10^{-8}$  m/cycle. Force shedding may be continuous by using analogue or digital computer. To fulfil this requirement normalized K-gradient (C) is used which is given by

$$C = \left(\frac{1}{K}\right) \cdot \left(\frac{dK}{da}\right) mm^{-1}$$

and it should be greater than  $-0.008 mm^{-1}$ . The normalized K-gradient and force ratio should be constant during the test. There is relation between crack size, normalized K-gradient and stress intensity factor which is given by

$$\Delta K = \Delta K_0 \cdot e^{[C(a-a_0)]}$$

where,  $\Delta K_0$  is the initial stress intensity factor range.

### 4.3.3 K increasing

K-increasing test is same as the K-decreasing test with having positive normalized K-gradient. Its main feature is its geometry independency. This procedure uses constant amplitude loading. The advantages of this test are the test time is reduced and  $da/dN$  data is evenly distributed.

### 4.3.4 Constant Load Test

This test procedure is suited for fatigue crack rate above the  $10^{-8}$ m/ cycle. In this method specimens are tested at constant force range and fixed loading variables (frequency and stress ratio). Changing the load variables may result some problems which is due to the transition phenomenon. The value of K is continuously increasing in this mode. To perform the constant load FCG test, first of all pre-crack parameters (pre-crack final size, pre-crack final P, pre-crack  $P_{max}$ , pre-crack final K, pre-crack  $K_{max}$ , pre-crack cycle completed) are entered after that final crack growth limit, value of constant load, stress ratio and frequency value are entered as input parameters.

## 4.4 FATIGUE CRACK GROWTH TEST OF 6351 AL ALLOY

FCG test of bulk and cryorolled samples are done using constant load method. The test is performed at frequency of 10 Hz and load ratio of 0.10. The samples used for this experiments study is shown in previous **Figure 2.15**.

Crack growth rate vs delta K curve is shown in **Figure 4.3**. From this plot Paris constant (C and m) are determined. This figure demonstrates that the FCG rate is significantly diminished for CR sample when contrasted with the ST Al 6351 alloy. And slow crack growth is observed in the CR 80 and CR 60 samples as comparison to ST samples. The increase in fatigue resistance is due to increase in plastic zone size at crack tip of CR samples.

The cryorolled samples provide higher fatigue resistance as compare of ST samples which have coarse grain structure. A high magnitude of  $\Delta K$  implies higher mechanical driving force to fatigue crack growth. It means, for same value of  $da/dN$ , a high value of K is required for CR samples. We know that cryorolling produce ultrafine grains which increase the yield and ultimate strength of materials and also prevent the surface damage due to intrusion and extrusion caused by fatigue and improve the fatigue resistance of cryorolled alloy. There are two ways by which ufg alloy provide resistance to cyclic deformation which are listed here (i) dislocation–dislocation interaction and (ii) dislocation–grain boundary interaction. In ufg (ultrafine grains) alloys fracture taken place because of the interaction of

propagating crack and grain boundaries and void created by grain boundary sliding. All the above mention factors are responsible for retardation in fatigue crack growth just in case of ufg Al 6351 alloy. CR specimens show ufg structures which have finely-dispersed precipitates of magnesium silicide and crack retardation is taken place due to interaction of crack–precipitate at the grain boundaries. whereas just in case of bulk 6351 alloy fatigue failure dominated by fatigue resistance of grains and grain boundaries has on influence of fatigue failures. So it is clear from figure that CR 40, CR 60 and CR 80 have higher fatigue resistance to crack propagation as compare to ST sample.

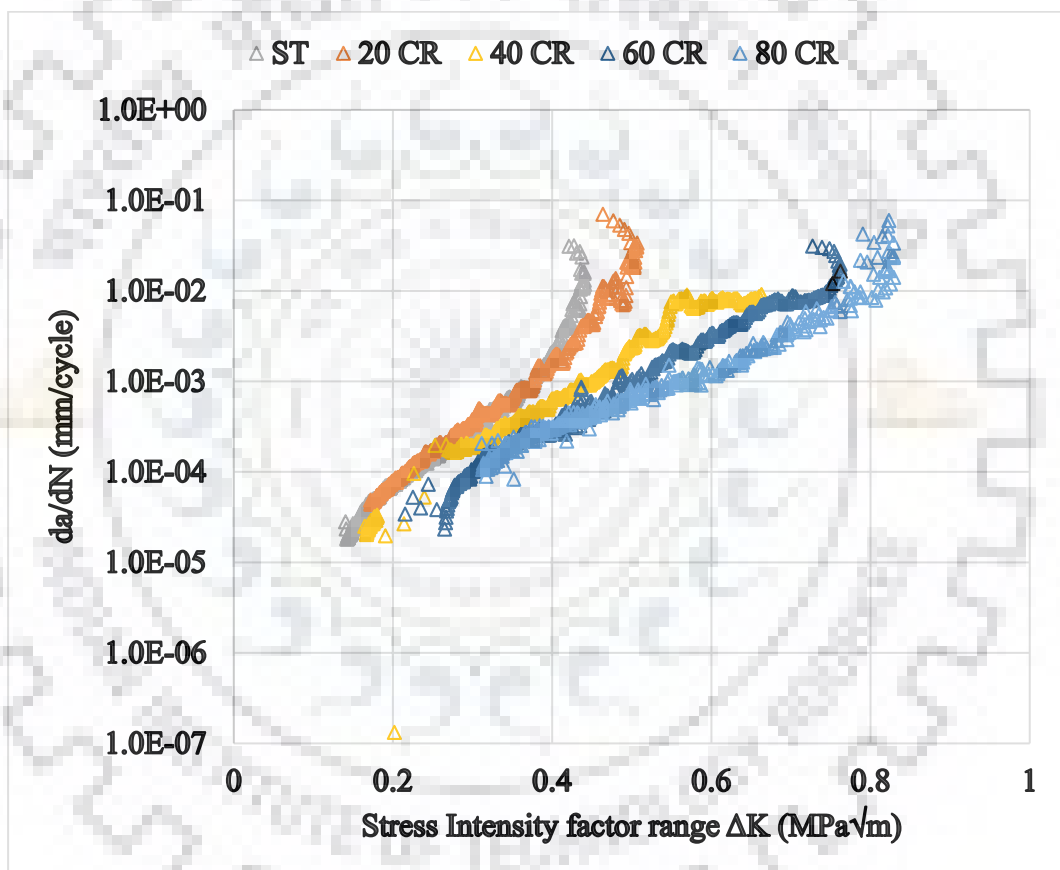
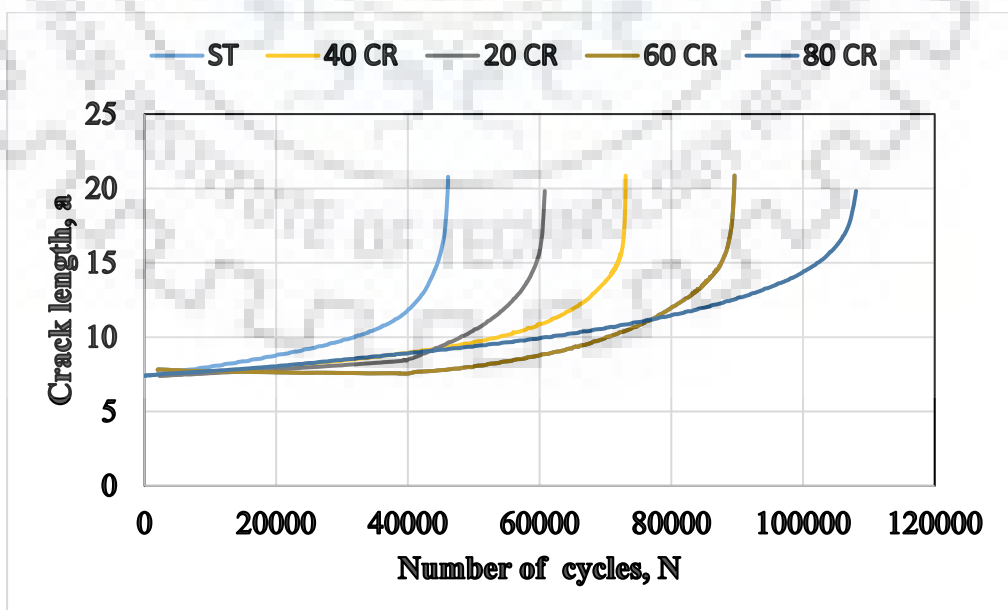


**Figure 4.3:** FCG curve for ST, CR 40, CR 60 and CR 80 AL alloy 6351

**Table 4.1** Value of Paris constants (C, m) for Al 6351 alloy at different thickness reductions

Sample Id	C	m
ST	$9.16 \times 10^{-12}$	6.15
CR20	$8.16 \times 10^{-11}$	5.84
CR 40	$5.21 \times 10^{-10}$	5.21
CR 60	$4.563 \times 10^{-9}$	4.83
CR 80	$5.83 \times 10^{-8}$	4.12

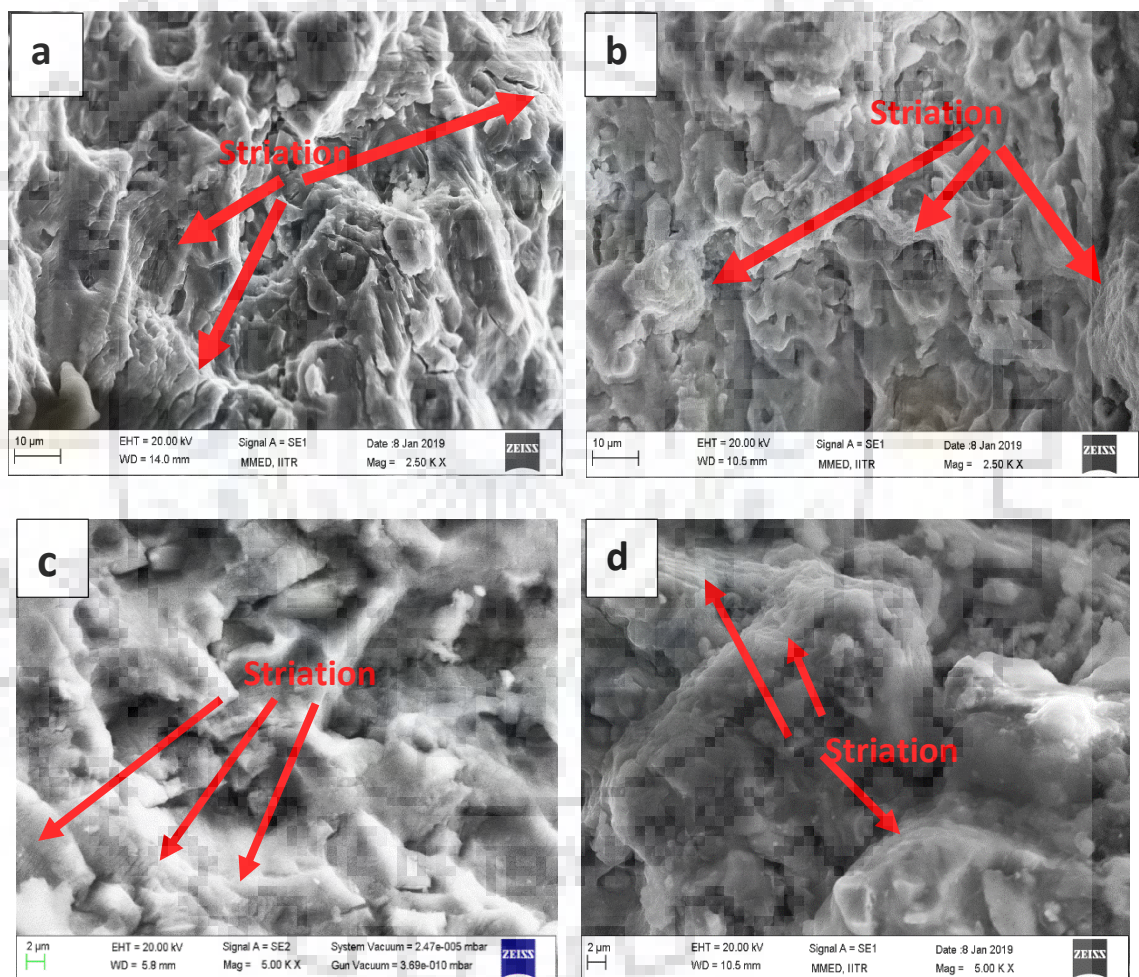
Fatigue crack growth test is done at constant load and crack length vs number of cycles (a vs N) curves is shown in figure for different thickness reduction through cryorolling ST, 20 CR, 40 CR, 60 CR and 80 CR. Initial crack length was 6.4 and specimen is pre-cracked up to 7.4 mm. After that crack growth is taken place under constant load and proceed to 22 mm because uncrack length of specimen was 28 mm. specimen is fractured at 22 mm crack length and divided into two parts. It is clear from curve (a vs N) that cryorolled specimen e.g. (20 % CR, 40 % CR, 60 % CR and 80 % CR) show higher fatigue life and fail after large number of cycles as compare to solution treated bulk alloy 6351. Solution treated sample (ST) failed after 46104 number of cycles while CR 20, CR 40, CR 60 and CR 80 failed after 60785, 73066, 89597 and 108059 number of cycles respectively. Crack length v/s number of cycles curve is shown in **Figure 4.4**.



**Figure 4.4:** Crack length v/s number of cycles curve

## 4.5 FATIGUE CRACK GROWTH FRACTOGRAPHY

Tested fracture surface of compact tension (CT) specimens are studied through Fe sem. Fractographs show that ductile striations are formed during fatigue crack growth of Al 6351 alloy and ductility is the necessary condition to form the ductile striations. From the fractograph, it is clear that striation width increase as we increase the percentage reduction in thickness of Al alloy 6351 through cryorolling. And gap among striations are smaller in case of ultrafine grains (ufg) as compare to solution treated or bulk alloy. We know that cryorolling produce ultrafine grains which provide better resistance to fatigue failure. Fatigue fractographs is shown in **Figure 4.5**.





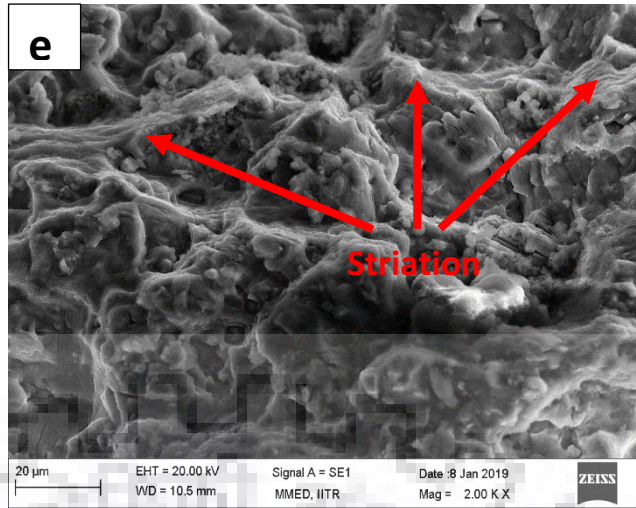


**Figure 4.5:** Fatigue crack growth fractographs of (a) ST (b) 20 % CR (c) 40 % CR (d) 60 % CR (e) 80 % CR Al alloy 6351

# CONCLUSION AND FUTURE SCOPE

### 5.1 CONCLUSION

6351 Al alloy is rolled for various thickness reduction at extremely low temperature (-196 °C) to boost the mechanical and fatigue properties. Different mechanical test such as tensile test, hardness test, fatigue crack growth tests are performed to characterize the effect of cryorolling on the 6351Al alloy. Microstructural characterization is done to support the result. Various conclusion is often drawn from results.

- The strength of as-received 6351 Al alloy is increased significantly after cryorolling process. The YS and UTS increased from 140 MPa to 365 MPa and 202 MPa to 415 MPa respectively.
- The ductility of cryorolled 6351 Al alloy is reduced from 20 % to 4 %, it is due to change in microstructure. But after aging treatment ductility is recovered up to 7 %.
- The hardness of the 6351 AL alloy has been increased from 68 Hv to 170 Hv. It is due to increase the dislocation density by cryorolling process.
- Fatigue crack growth study shows that cryorolled samples of 6351 Al alloy sustain higher number of cycles as compare to bulk 6351 Al alloy.
- The optimum aging condition for Al 6351 alloy is found to be 100°C and 12 hours.
- Paris law constants for bulk (ST) and CR 80 6351 AL alloy are found to be  $C=9.16 \times 10^{-12}$ ,  $m=6.15$  and  $C=4.12$ ,  $m= 5.83 \times 10^{-8}$  respectively.

### 5.2 FUTURE SCOPE

6351 Al alloy is the future material for aircraft. However, the following work can also be performed on this material,

- The effect of forging and extrusion can be investigated.
- The effect of aging on room temperature rolled 6351 Al alloy can be investigated to boost the mechanical properties.
- Impact behavior of bulk 6351 alloy can be studied.
- Impact behavior of room temperature rolled and cryorolled 6351 Al can be investigated.

- High and low cycle fatigue behavior of bulk and cryorolled 6351 Al alloy can be performed.
- Creep behavior of rolled and cryorolled 6351 Al alloy can be investigated.



## **REFERENCES**

- [1] Hafirman Idrus, M. Afendi, Wong Chun Hoe, "Fatigue crack initiation and growth of aluminium alloy with anisotropy effects," *Key Engineering Materials*, vol 594-595, pp. 1105-1111, 2013.
- [2] Omer G. Bilir and Metin Harun, "Effect of stress ratio on the rate of growth of fatigue cracks in 1100 Al-alloy," *Engineering Fracture Mechanics*, vol 37, 6, pp. 1203-1206, 1990.
- [3] Robert E. Zinkham, "Anisotropy and thickness effects in fracture of 7075-T6 and T651 aluminum alloy," *Engineering Fracture Mechanics*, vol 1, pp. 275-289, 1968.
- [4] Nelson. F. G, Schilling, P. E and Kaufman. J. G, "The effect of specimen size on the results of plane-strain fracture toughness tests," *Engineering Fracture Mechanics*, vol 4, pp. 33-50, 1972.
- [5] Mills. W. J, and Hertzberg. R. W, "The effect of sheet thickness on fatigue crack retardation in 2014-T3 aluminum alloy," *Engineering Fracture Mechanics*, vol. 7, pp. 705-711, 1975.
- [6] Samer Mahmoud and Kaven Lease, "The effect of specimen thickness on the experimental characterization of critical crack-tip-opening angle in 2024-T351 aluminum alloy," *Engineering Fracture Mechanics*, vol. 70, pp. 443-456, 2003.
- [7] Samer Mahmoud and Kaven Lease, "Two-dimensional and three-dimensional finite element analysis of critical crack-tip-opening angle in 2024-T351 aluminum alloy at four thicknesses," *Engineering Fracture Mechanics*, vol. 71, pp. 1379-1391, 2004.
- [8] Kermanidis, A.T and Pantelakis, Sp. G, "Prediction of crack growth following a single overload in aluminum alloy with sheet and plate microstructure", vol.78, pp. 2325-2337, 2011.
- [9] R. Jayaganthan, S.K. Panigrahi, *Mater. Sci. Forum* 584–586 (2008) 911–916.
- [10] R. Jayaganthan, S.K. Panigrahi, *Mater. Sci. Forum* 584–586 (2008) 734–740.
- [11] X.M. Li, M.J. Stranik, *Mater. Sci. Technol.* 17 (2001) 1324–1328.
- [12] J. Li, Z. Peng, C. Li, Z. Jia, W. Chen, Z. Zheng, *Trans. Nonferrous Met. Soc. China* 18 (2008) 755–762.
- [13] J.C. Williams, E.A. Starke, *Acta Mater.* 51 (2003) 5775–5799.

- [14] D. Steglich, W. Brocks, J. Heerens, T. Pardoen, *Eng. Fract. Mech.* 75 (12) (2008) 3692–3706.
- [15] P. Das, R. Jayaganthan, I.V. Singh, *Mater. Des.* 32 (3) (2011) 1298–1305.
- [16] P. Das, R. Jayaganthan, T. Chowdhury, I.V. Singh, *Mater. Sci. Forum* 683 (2011) 81–94.
- [17] P. Cavaliere, *Int. J. Fatigue* 31 (2009) 1476–1489.
- [18] L. Collini, *Eng. Fract. Mech.* 77 (2010) 1001–1011.
- [19] L. Collini, *Procedia Eng.* 2 (2010) 2065–2074.
- [20] A. Vinogradov, *J. Mater. Sci.* 42 (2007) 1797–1808.
- [21] ASTM Standard E8/E8M, 2009, ASTM International, West Conshohocken PA 2009; doi:10.1520/E0008-E0008M-09, [www.astm.org](http://www.astm.org).
- [22] ASTM Standard E468-90 (2004) e1, ASTM International, West Conshohocken PA 2004; doi:10.1520/E0468-90R04E01, [www.astm.org](http://www.astm.org).
- [23] ASTM Standard E466-07, ASTM International, West Conshohocken PA 2007; doi:10.1520/E0466-07, [www.astm.org](http://www.astm.org).
- [24] ASTM Standard E647-08e1, ASTM International, West Conshohocken PA 2008; doi:10.1520/E0647-08E01, [www.astm.org](http://www.astm.org).
- [25] P. Vasudevan, B.R. Satyan, *Indian J. Technol.* 12 (1974) 475–478.
- [26] R. Jayaganthan, S.K. Panigrahi, *Mater. Lett.* 62 (2008) 2626–2629.
- [27] H. Mughrabi, H.W. Hoppel, *Int. J. Fatigue* 32 (2010) 1413–1427.
- [28] C. Xu, Q. Wang, M. Zheng, J. Li, M. Huang, Q. Jia, J. Zhu, L. Kunz, M. Buksa, *Mater. Sci. Eng. A* 475 (2008) 249–256.
- [29] H. Mughrabi, H.W. Hoppel, M. Kautz, *Scripta Mater.* 51 (8) (2004) 807–812.
- [30] B.B. Verma, J.D. Atkinson, M. Kumar, *Bull. Mater. Sci.* 24 (2) (2001) 231–236.
- [31] B.F. Jogi, P.K. Brahmkumar, V.S. Nanda, R.C. Prasad, *J. Mater. Process. Technol.* b201 (1–3) (2008) 380–384.

- [32] ASTM Standard E1820-09e1, ASTM International, West Conshohocken PA2009; doi:10.1520/E1820-09E01, www.astm.org.
- [33] J Xie, X. Wu, Y. Hong, *Scripta Mater.* 57 (2007) 5–8.
- [34] A.K. Vasudevan, K. Sadananda, K. Rajan, *Int. J. Fatigue* 19 (93) (1997) 151–159.
- [35] Y. Estrin, A. Vinogradov, *Int. J. Fatigue* 32 (6) (2010) 898–907.
- [36] Y.G. Kim, B. Hwang, S. Lee, C.W. Lee, D.H. Shin, *Mater. Sci. Eng. A* 504 (2009) 163–168.
- [37] L.W. Meyer, K. Sommer, T. Halle, M. Hockauf, *J. Mater. Sci.* 43 (2008) 7426–7431
- [38] S. Maitra, G.C. English, Environmental factors affecting localized corrosion of 7075-t7351 aluminum alloy plate, *Metall. Mater. Trans. A* 13 (1982) 161e166.
- [39] X. Yan, S. Liu, W. Long, J. Huang, L. Zhang, Y. Chen, The effect of homogenization treatment on microstructure and properties of ZnAl15 solder, *Mater. Des.* 45 (2013) 440e445.
- [40] G. Ben-Hamu, D. Eliezer, K.S. Shin, The role of Mg<sub>2</sub>Si on the corrosion behaviour of wrought MgZnMn alloy, *Intermetallics* 16 (2008) 860e867.
- [41] S. Katsas, J. Nikolaou, G. Papadimitriou, Corrosion resistance of repair welded naval aluminium alloys, *Mater. Des.* 28 (2007) 831e836.

# Turnitin Originality Report

Processed on: 11-May-2019 11:20 IST  
 ID: 1128725693  
 Word Count: 11063  
 Submitted: 1

M.Tech Thesis By Gayanendra Saini

Similarity Index

13%

#### Similarity by Source

Internet Sources: 6%  
 Publications: 9%  
 Student Papers: 8%

2% match (student papers from 30-Apr-2019)

[Submitted to Indian Institute of Technology Roorkee on 2019-04-30](#)

1% match (Internet from 14-Jul-2018)

[http://lutpub.lut.fi/bitstream/handle/10024/156020/mastersthesis\\_krekhovetckii\\_nikita.pdf?isAllowed=y&sequence=1](http://lutpub.lut.fi/bitstream/handle/10024/156020/mastersthesis_krekhovetckii_nikita.pdf?isAllowed=y&sequence=1)

1% match (student papers from 24-Apr-2019)

[Submitted to Indian Institute of Technology Patna on 2019-04-24](#)

1% match (Internet from 07-Mar-2016)

<http://iaeme.com/MasterAdmin/UploadFolder/30120140502012/30120140502012.pdf>

1% match (Internet from 27-Jan-2015)

[http://www.aryatajhiz.com/userfiles/ASTM/E647\\_00\\_RTY0NW.pdf](http://www.aryatajhiz.com/userfiles/ASTM/E647_00_RTY0NW.pdf)

1% match (student papers from 06-Apr-2019)

[Submitted to Indian Institute of Technology Roorkee on 2019-04-06](#)

< 1% match (publications)

[Stark, H.L. "Crack propagation at constant load and room temperature in an extruded aluminium", Engineering Fracture Mechanics, 1988](#)

< 1% match (publications)

[J.W.H. Price, R.N. Ibrahim, D. Ischenko. "Sustained load crack growth leading to failure in aluminium gas cylinders in traffic", Engineering Failure Analysis, 1997](#)

< 1% match (publications)

[Sushanta Kumar Panigrahi, R. Jayaganthan. "Effect of ageing on microstructure and mechanical properties of bulk, cryorolled, and room temperature rolled Al 7075 alloy", Journal of Alloys and Compounds, 2011](#)

< 1% match (publications)

[Amit Joshi, K.K. Yogesha, R. Jayaganthan. "Influence of cryorolling and followed by annealing on high cycle fatigue behavior of ultrafine grained Al 2014 alloy", Materials Characterization, 2017](#)

< 1% match (publications)

[Sushanta Kumar Panigrahi, R. Jayaganthan. "Development of ultrafine grained high strength age hardenable Al 7075 alloy by cryorolling", Materials & Design, 2011](#)

< 1% match (publications)

[Patelakis, Sp.G.. "Fatigue crack growth retardation assessment of 2024-T3 and 6061-T6 aluminium specimens", Theoretical and Applied Fracture Mechanics, 199501/02](#)

< 1% match (Internet from 12-Jun-2009)

[http://www.caricom-fisheries.com/website\\_content/publications/documents/Final\\_Report\\_Effects\\_of\\_Liberalization\\_and\\_Trade\\_Related\\_Policies.p](http://www.caricom-fisheries.com/website_content/publications/documents/Final_Report_Effects_of_Liberalization_and_Trade_Related_Policies.p)

< 1% match (publications)

[Vineet Kumar, I.V. Singh, B.K. Mishra, R. Jayaganthan. "Experimental Investigation of Fatigue Behavior of CR and RTR 6082 Al-alloy", Procedia Materials Science, 2014](#)

< 1% match (publications)

["Proceedings of the 15th International Conference on Environmental Degradation of Materials in Nuclear Power Systems — Water Reactors", Springer Nature, 2016](#)

< 1% match (publications)

[Guo, Ran, En Qiang Lin, Rui Chun Duan, Gerard Mesmacque, and Abdelwaheb Amrouche. "Study of Fretting Fatigue Crack Initiation For Riveted Al 6xxx Components", Advanced Materials Research, 2008.](#)

< 1% match (publications)